Fatigue Life Estimation of Vehicle Mounted Components Using Full Car Suspension Bond Graph Model

Author

Waqas Ahmed

2009-NUST-MsPhD-Mech-10

Supervisor

Dr. Aamir A.Baqai

DEPARTMENT OF MECHANICAL ENGINEERING

COLLEGE OF ELECTRICAL & MECHANICAL ENGINEERING

NATIONAL UNIVERSITY OF SCIENCES AND TECHNOLOGY

ISLAMABAD

SEPTEMBER, 2013

Fatigue Life Estimation of Vehicle Mounted Components Using Full Car Suspension Bond Graph Model

Author

Waqas Ahmed

2009-NUST-MsPhD-Mech-10

A thesis submitted in partial fulfillment of the requirements for the degree of

M.Sc. Mechanical Engineering

Thesis Supervisor:

Dr.Aamir A.Baqai

Thesis Supervisor Signature: _____

DEPARTMENT OF MECHANICAL ENGINEERING

COLLEGE OF ELECTRICAL & MECHANICAL ENGINEERING

NATIONAL UNIVERSITY OF SCIENCES AND TECHNOLOGY,

ISLAMABAD

SEPTEMBER, 2013

Declaration

I certify that research work titled "*Fatigue Life Estimation of Vehicle Mounted Components Using Full Car Suspension Bond Graph Model"* is my own work. The work has not been presented elsewhere for assessment. Where material has been used from other sources it has been properly acknowledged / referred.

Signature of Student

Waqas Ahmed

2009-NUST-MsPhD-Mech10

Copyright Statement

Acknowledgements

I am thankful to you, my Creator Allah Subhana-watala, who is the source of all the guidance, strength and courage for me.

I am profusely thankful to my beloved parents for all their encouragement and support during the course of this challenging period.

Special Thanks to my supervisor Dr Aamir Ahmed Baqai for his help throughout my thesis. Without his supervision; I would never have accomplished this work

I would also like to pay special thanks to Raja Amir Azim for all the help he provided me during the course of this work. The course on System Dynamics taught by him was a valuable tool that helped me to understand Bond Graph methodology.

Thanks to Dr. Hassan Aftab, Dr. Imran Akhtar for being on my thesis guidance and evaluation committee.

I would also like to express my gratitude to my office seniors whose support allowed me to pursue my research work without any worry.

Finally, I would like to express my gratitude to all the individuals who have rendered valuable assistance to my study.

Dedicated to my beloved parents and adored siblings whose tremendous support and cooperation led me to this wonderful accomplishment.

ABSTRACT

Fatigue life of vehicle mounted components is dependent on a number of factors like mounting location, suspension parameters, component design, and anti-vibration mount properties. A study of influence of these parameters on component fatigue life will greatly help in establishing the most suitable values of these parameters for a given mounting problem. The existing techniques to determine the fatigue life of vehicle mounted components are not used to study fatigue life variation by changing the above mentioned parameters as the practice is time consuming and costly with these techniques. This calls for the development of an efficient framework by which such a study can be carried out. In the present research work such a framework is developed by using the bond graph method of modeling and simulation. With the help of this framework, a rough estimation of fatigue life of vehicle mounted components can be made, for various parameter values, in considerably less time as compared to existing techniques of fatigue life determination. Thus the variation occurring in the component fatigue life by varying parameter values can be known, which allows determination of most appropriate values of these parameters to get maximum fatigue life of vehicle mounted components. Once the suitable parameter values have been established, the detailed fatigue life of component can be determined using existing techniques. A full car suspension model is generated using bond graph method, and after validation of the model it is augmented to include a component mounted on vehicle body at four points. To simulate actual travel conditions, a road profile is generated and is provided as input to the model, which provides the load values acting at the component mounting points. The dynamic stresses generated in component are known by performing finite element analysis of the component with known load values. From these dynamic stresses a preliminary fatigue life of component is calculated using Rainflow counting algorithm and Palmgren-Miner's rule. The whole process is repeated at four mounting locations on vehicle body and the variation occurring in component fatigue life by varying mounting location is established. Finally, modal analysis of the full car suspension is carried out and the variation in fatigue life is related to the variation of modal displacements of various points on vehicle body.

Table of Contents

List of Figures

List of Tables

CHAPTER 1: INTRODUCTION

The research work in this dissertation has been presented in two parts. First part deals with the generation of bond graph model of full car suspension with mounted component at four mounting points. Simulation of this model with known road profile provides load values at four mounting points of the component. In the second part, the dynamic stresses generated in the component due to random load values acting at component mounting points are determined by performing transient stress analysis of the component, and fatigue life of the component is estimated from these stresses by using Rainflow counting algorithm and Miner's rule.

1.1 Automotive Suspension System

Automotive suspension is a system of springs, shock absorbers, actuators and linkages that connect the vehicle body to the axles [1]. The vehicle body is referred to as the sprung mass, while the axles are referred to as the unsprung mass. The sprung mass consists of the passenger compartment, engine and other mechanical parts. The unsprung mass refers to the vehicle tires and wheels.

Automobile suspension system is a crucial part of any vehicle as it performs the essential function of vibration isolation, thus mitigating the vibration level reaching the passenger and mounted components. It also improves vehicle road holding ability by increasing the frictional contact between tires and road. Greater vibration levels are a source of discomfort for the passengers sitting in the compartment as well as a source of damage for the various sensitive components attached to the vehicle body at various points for various purposes. Reduced road holding conveys less "feel" of road surface to the driver and also deteriorates tire grip on road, as a result of which vehicle loses traction.

In the context of vehicles carrying various components/equipements, such as military vehicles carrying heavy and sensitive payload, autonomous guided vehicles (AGVs), and robotic rovers operating on surface of other planets with sensitive instrumentation mounted on board; ensuring safety of the mounted components against fatigue failure is essential. Since vibration is essentially dynamic loading, which after transmission to the mounted components causes dynamic stresses to be generated in the component, ultimately causing components to fail due to fatigue; if these stresses are not below the endurance limit of the component material. The current practice is to know the fatigue life of mounted components

using various experimental and CAD based approaches. Study of variation of fatigue life by changing various parameters that influence the fatigue life of mounted components; like suspension parameters, mounting location and anti vibration mount properties can help to establish optimum values of these parameters for maximum fatigue life of component. The techniques employed for fatigue life determination of vehicle mounted components are not used for the purpose as the practice becomes time consuming and costly with these techniques.

1.2 Scope of Present Work

As stated earlier, the various methods used to determine fatigue life of vehicle mounted components are not used to study the variation occurring in fatigue life of the components due to change of various parameters that affect the component fatigue life. In case of experimental methods, determination of fatigue life is made by acquiring real time vibration data from actual vehicle travel and this vibration data is used to know the dynamic stresses generated in the component by carrying out finite element (FE) analysis of the component, either using time domain or frequency domain approach. The fatigue life is then determined from these stresses. In some cases, stresses are measured directly by making use of strain gauges. Study of fatigue life variation by such methods will become time consuming and costly, as, if any change like change of component location, or change of suspension parameters is done as it will require making major changes in experimental setup.CAD based approaches rely on CAD model of vehicle, which when simulated with actual road profile gives vibration data at any location on vehicle. Since a detailed vehicle model has to be generated, study of fatigue life variation by changing vehicle characteristics means making major changes in design of CAD model, and this makes the CAD based approach unsuitable to study fatigue life variation of vehicle mounted components.

In the light of these facts it is realized that an efficient framework need to be developed to study fatigue life characteristics of vehicle mounted components. Detailed fatigue life evaluation, which makes use of dynamic stress data for a considerable period of time, is not required to be done. Only, the variation occurring in fatigue life has to be checked, so estimated fatigue life values calculated using a few seconds of stress data will be used. Thus the time required to calculate vibrational loads for thousands of seconds of vehicle travel is saved. The first task in the development of required framework is to come up with a model of full car suspension with mounted component. The model must be generated with a modeling technique that overcomes the limitations present in the experimental and CAD

based approaches i-e, any kind of modification/augmentation in the physical system like changing component mounting location, changing number of attachment points of component, or changing suspension parameters of vehicle must be incorporated in the model without the need to make major changes in the model. The technique must be used with the help of which such changes can be incorporated merely by changing parameter values, and the structure of model remains intact. After generation of model actual travel conditions need to be simulated by providing road profile as input to vehicle model, which provides the vibration load values at component mounting locations. From these load values a preliminary finite element analysis of the component provides the dynamic stress values which are can be used to estimate fatigue life. The repetition of whole process by changing component mounting location gives the component fatigue life variation with the variation of mounting location. The variation of fatigue life by changing other parameter values like suspension properties of vehicle and anti-vibration mount characteristics can well be done using the current framework. However, present study of fatigue life variation is performed only for various mounting location of component.

1.3 Objectives of Study

The objectives of this study can be summarized in the form of following points:

1. To develop a framework for mapping vibration from road to attachment points of vehicle mounted components.

2. Use the random vibration values at the component mounting points to perform the FE analysis of attached part and come up with dynamic stress values and an estimated fatigue life at a particular location.

3. Study of variation of component fatigue life with variation of component mounting location.

4. Finally, establishment of relationship between component fatigue life and the modal displacements of component mounting points, and identification of most appropriate mounting location on vehicle body, using the relationship.

1.4 Literature Review

A vast amount of literature review has been done regarding the vehicle suspension modeling, random road profiles, semi active suspension and fatigue behavior of metals.

Researchers have mostly focused their work toward the improving the ride quality and handling of the vehicles using quarter car, half car and full car models.Usually,their works involve generation of active and semi active suspensions to achieve desired characteristics in the vehicle suspension.Gallispie[2] has studied the bounce characteristics of a quarter car suspension model.Yue[1] has studied various control techniques for the full car model like LQR,LQG for improving the ride and handling.Shirahatti et al.[3] have studied full car suspension characteristics using the LQR control strategy tuned using genetic algorithms. The work of Abramov et al.[4] deals with studying full car suspension characteristics using semi active suspension and rough road profile.Adibi and Rideout[5] have generated full car seven degree of freedom model using the bond graph method and converted it to active suspension system.

The fatigue damage which occurs in vehicle mounted components is due to random vibration and thus random or non-uniform dynamic stresses. Usually, for accurate fatigue life calculation, stress or fatigue data of the order of thousands of seconds is used.Leser et al[17] have described a statistical approach by which a given loading data can be reconstructed and extended. The fatigue analysis due to random loading history is broadly divided into two main classes. The analysis which makes use of the time signal of load data to know time signal of stress data is known as time based approach. While the analysis which makes use of frequency signal of load data to know the frequency based stress results falls in the category of frequency based approach. Khan et al[6] have carried out fatigue life analysis of auxiliary heater bracket mounted to truck body using real time vibration data. A closely related work is done by Cheng and Crull[7],fatigue life estimation of an ECM motor assembly has been carried out using experimental vibration data. In both of these works, frequency domain approach is used. Power spectral density (PSD) of real time vibration data is applied to CAD model of component and the finite element analysis provides a statistical distribution of generated stresses. This analysis can be performed quickly as most of FE packages have built in modules to perform such kinds of analysis. A similar analysis is done in reference[16], in which the fatigue life of a girder assembly is carried out.

Ariduru [8] has carried out fatigue life estimation of a notched cantilever beam using response vibration data of beam due to random input excitations. Both time domain and

frequency domain approaches have been used. Time domain approach uses Rainflow cycle counting algorithm to know number of cycles present in stress spectrum. Frequency domain approach makes use of Dirlik's approach[19] to know number of stress cycles . Fatigue life is then calculated using Palmgren-Miner's rule of fatigue damage. This frequency domain analysis takes more time as compared to that of refrences [6] and [7].However, the approach of references [6] and [7] is used for the case when we are provided with a recommended loading curve known as general minimum integrity exposure curve.

The work of Tahami et al[9] deals with determining fatigue life of suspension support of an off-road vehicle, using time domain approach. This work relies on the dynamic simulation of a CAD vehicle model by known road profile in ADAMS software. The load values provided by ADAMS are then used to know dynamic stresses generated at suspension support by simulating a FE model of suspension support. The fatigue life calculation then follows the time domain approach as described in reference[8].

The work of Kagnici[15] makes use of frequency domain approach to determine fatigue damage occurring in body panels of a minivan. The body portions of the vehicle that get most of the fatigue damage are identified. Rather than using statistical stress distribution to calculate fatigue life as in references[6] and [7], this method makes use of Craig-Bampton modes of vehicle. Time histories of deformation of Craig-Bampton modes are processed in NCODE Design life software to calculate fatigue life.

A review of previous research work makes it apparent that the frequency domain approach is computationally more efficient, as compared to time domain approach. However, later we shall see that for the purpose of calculation of dynamic stresses for components which have multiple attachment points on vehicle bodies, frequency domain approach does not work.

1.5 Methodology Used

The methodology used in the present thesis can be summarized in the form of a flow chart

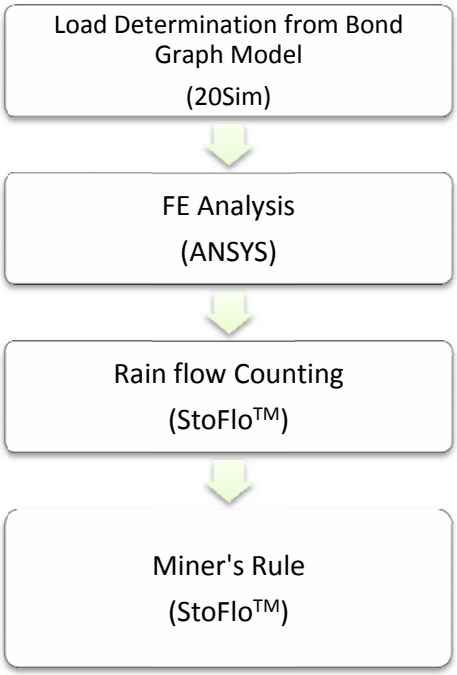

The bond graph model of the full car suspension with attached component provides the load values acting at the mounting points of the component. These load values are then used to perform the finite element analysis of the mounted component in ANSYS.The dynamic stress values thus obtained are then used to perform the fatigue life estimation of the component using Rain flow counting algorithm and Miner's rule of cumulative fatigue damage.

1.6 Outline

The basic steps of this study are discussed in the form of chapters that describes the complete explanation and description of the related work that has been carried out to accomplish the task.

Chapter 1 is an introduction to the problem. Automobile suspension system is explained and the need to carry out the fatigue life study of vehicle mounted components is explained. Brief overview of the literature survey carried out is also given.

Chapter 2 explains the main concepts associated with bond graph method of modeling and simulation.

In Chapter 3, modeling of automobile suspension of full car is carried out. Starting with the quarter car suspension, we proceed to model the full car suspension using bond graph method. The model is verified and is then augmented to include a component mounted on the vehicle body at four points.

In Chapter 4, a time signal of road profile is generated which is used as the input to the vehicle suspension model. Detailed procedure involved in generation of time signal of road profile, for a vehicle travelling at 60km/h, from the PSD data is explained.

Chapter 5 deals with the details of the fatigue life calculation. The load values obtained after simulation of the bond graph model with road profile are used to perform the finite element analysis of the CAD model of attached component which gives us the dynamic stresses generated in the component, and fatigue life is then calculated from these stress values.

In Chapter 6, recommendations for the future work are proposed and summarization of the current work is being carried out.

CHAPTER 2: A BRIEF INTRODUCTION TO BOND GRAPH

2.1 Modeling of Multi Domain Systems Using Bond Graphs

Bond graph is a graphical method of modeling and simulation of dynamic systems based on energy and information flow between system components. Using bond graph method system models can be constructed using a uniform notation for all types of physical systems[14].Systems from different physical domains like mechanical, electrical, hydraulic, as well as mixed domain systems can effectively be modeled using bond graph method. Because of this bond graph has become one of the most powerful methods of modeling mechatronics systems. A bond graph model of a dynamic system is also known as energy based model.

The underlying theme of the bond graph method is that the physical systems, no matter what domain they belong to, are similar in the sense that the working of all physical systems involves power exchange between various system components. Change of physical domain merely changes the form of power flow between the systems components.

2.2 A Simple Example of Bond Graph Model

2.2.1 Mass Spring System and RL Circuit

In order to explain the modeling procedure using the bond graph method and to show the equivalence of different physical domains, an example of modeling of a simple mechanical and an electrical system is given:

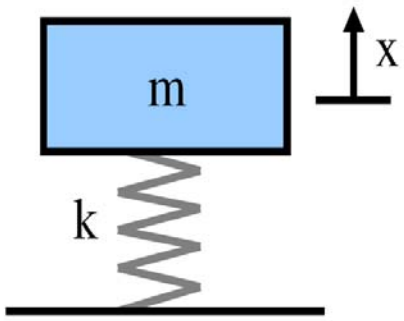

Figure 2-1: A spring mass system

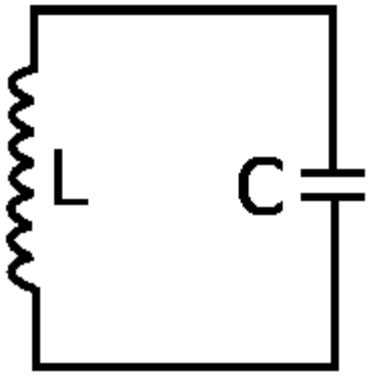

Figure 2-2: An RLC circuit

The Fig 2-1 and Fig 2-2 above, shows a very simple mechanical system consisting of a mass connected to a spring and it's equivalent electrical system; consisting of a capacitor and an inductor. It is not clear at this point how these two physical systems are equivalent. However as both of these systems are modeled using the bond graph method, the similarity of the two systems becomes clear. The Bond Graph model is shown in Fig 2-3:

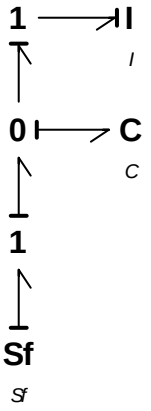

Figure 2-3: A bond graph model of spring mass system

In both the systems there are two components; spring element and inertia element in the mechanical system, and capacitor and inductor in the electrical element. As stated in the start, all physical systems involve power exchange between components or power flow from one component to another. In the mechanical system above, the spring receives a power input (velocity or flow) which flows from spring to the mass. Since power is the product of force and velocity. If force is given as input to any element, say spring, then velocity will be calculated by it and vice versa. There are two facets related to both the electrical system and it's mechanical

counterpart by which the equivalence of the two systems can be established. First, both systems involve power flow. In mechanical system the power input signal is composed of velocity and force and in electrical system it is composed of current and voltage.Second,both the systems are composed of same elements ie,capacitive element and the inertia element. In mechanical system capacitive element is the spring, while in electrical system the capacitor is the capacitive element. Similarly, the inertia element in the mechanical system is the mass, while in electrical system; the inductor is the inertia element.

2.2.2 Components and Constitutive Relations

The above two points definitely require explanation. First we come to power. As we know that for a mechanical system:

$$Power = Force \times Velocity \tag{2.1}$$

And for an electrical system:

$$Power = Voltage \times Current \tag{2.2}$$

The current is flow of charge in a unit time and velocity is flow in a unit time. The two are equivalent. Voltage is the potential which causes this flow just like force causes the flow in the mechanical systems. Thus we can say that voltage is similar to force and current is similar to velocity. The consequence of applying voltage between two points is to make charge to flow between those points and the consequence of applying force is to make it to undergo a displacement.

Now we come to the components of the two systems. How the components from two different domains have similarity. The capacitor element which receives the input as current accumulates the charge. The equation governing the behavior of capacitor or the constitutive equation of capacitor is:

$$e = \frac{1}{C}\int V = \frac{q}{C} \tag{2.3}$$

Where q is the charge which is obtained by integrating the input velocity. The output is thus the force and depends on the capacitance or compliance C and the current applied. In the

mechanical system the input velocity is on the spring. By Hook's law we know that for a linear spring:

$$F = kx \tag{2.4}$$

K is the stiffness of the spring and the x is the displacement of the spring or the spring deflection, which, as in case of capacitor is obtained by integrating the flow or velocity reaching it. The inverse of the k is C or compliance. Thus we can write;

$$F = \frac{x}{C} \tag{2.5}$$

Thus the mechanical spring and the electrical capacitor are similar. Both receive the velocity as input, integrate it and return the force information.

Next the inductor element or inertia element is considered. It receives the force, integrates it and returns the information about the flow. The equation governing the behavior of the inertia element is:

$$f = I\frac{\int a}{I} \tag{2.6}$$

Here a is the acceleration which gets integrated and thus flow or velocity information f is returned. I is the inertia value. In the Fig 2-3, input is the velocity represented by Sf, the capacitor element takes this velocity information as input and returns the information about effort or force, the inertia element takes this information about effort and returns the information about velocity with which the inertia element will move. The equations (2.6) and (2.3) respectively govern the behavior of inertia element and capacitor element.

A third element in common use in the physical systems is the resistive element. It takes the form of resistor in electrical circuit and damper in mechanical system. It's governing equation is written as:

$$e = fR \tag{2.7}$$

Here f is the flow which when multiplied by the resistance R gives the value of effort. In electrical domain this equation takes the form of Ohm's Law. Having established the equivalence

between the physical systems from various domains, it becomes essential that a common nomenclature be used to identify the physical system components and power variables.

Another element used in bond graph methodology is the transformer element. Simply stated it transforms effort to moment and vice versa. The constitutive element of transformer is written as:

$$e2 = me2 \tag{2.8}$$

$$f1 = mf2 \tag{2.9}$$

Simply stated f2 is angular velocity achieved when acted upon by transformation ratio m concerts to linear velocity f1.Similarly in case of effort, e2 is the moment which is obtained when linear force e1 gets multiplied by m.

2.3 Equivalence of Power Variables and Components from Various Domains

The power variables from the various domains are identified as given in table 2-1 below:

Table 2-1: Effort and flow signal forms in various domains

DOMAIN	EFFORT	FLOW
Mechanical Translation	Force	Velocity
Mechanical Rotation	Torque	Angular Velocity
Electrical	Voltage	Current
Hydraulic	Pressure	Volume Flow Rate

The components are identified as given in the table 2-2:

Table 2-2: Component forms in various physical domains

DOMAIN	CAPACITIVE ELEMENT	INERTIA ELEMENT	RESISTIVE ELEMENT
Mechanical Translation	Spring	Mass	Damper
Mechanical Rotation	Torsion Spring	Moment of Inertia	Rotational Damper
Electrical	Capacitor	Inductor	Resistor

2.4 Vector Bond Graphs

So far the discussion has been focused on scalar or 1D bond graphs.1D bond graphs can accurately represent models of simple dynamic systems, however as systems get complex it is not possible to represent them accurately with 1D bond graphs. Vector or multi bond graphs are employed in such cases. The main difference between scalar and vector bond graphs is explained in the following points:

1. The signal flow between various elements in a vector bond graph is vector representing the power value in x, y and z directions respectively.

2. The values assigned to various elements in vector bond graphs are represented as 3 by 3 matrices. The matrix contains the parameter values in the x, y and z directions.
3. In case of transformation simple scalar multiplication cannot be used; rather vector multiplication will take place. For example; the equation will be written for vector bond graph in the following manner:

$$f2 = f1 \times m \tag{2.10}$$

Here × represents cross product.f1 and m are both vectors having 3 rows and 1 column. Thus three flow values in x, y and z directions are obtained.f2, f1 and m can be written in matrix form as:

$$\begin{matrix} f2x \\ f2y \\ f2z \end{matrix} = \begin{matrix} f1x \\ f1y \\ f1z \end{matrix} \times \begin{matrix} mx \\ my \\ mz \end{matrix} \tag{2.11}$$

The element I can be written in matrix form as:

$$\begin{matrix} Ixx & Ixy & Ixz \\ Iyx & Iyy & Iyz \\ Izx & Izy & Izz \end{matrix} \tag{2.12}$$

Similarly C, R elements can be written. Usually, diagonal values are given as the values of off diagonal parameters are mostly zero. The division occurring in the constitutive equations of elements is replaced by inverse matrix.

CHAPTER 3: MODELING OF SUSPENSION SYSTEM

In this chapter, a full car suspension will be modeled using bond graph. The development of full car suspension bond graph model is carried out in a systematic manner, starting with a quarter car suspension analytical model and developing it's bond graph model. The two models are then compared for the same type of road inputs to show the equivalence of two models. The same procedure is then repeated for the half car and finally for full car suspension model. In this way the evolution of the full car suspension dynamics becomes clear. After the development of the full car suspension using bond graph, the same model is developed using vector bond graph. Once the full car suspension model is available it is validated by comparing results with the results of a full car suspension model available in literature and then the model is modified to include a component mounted to vehicle body at four attachment points

3.1 Quarter Car Suspension

A quarter car suspension models is the simplest representation of vehicle suspension system as it includes only the bounce motion of the vehicle. This model provides a useful insight into suspension behavior. Fig 3-1 shows a quarter car model.

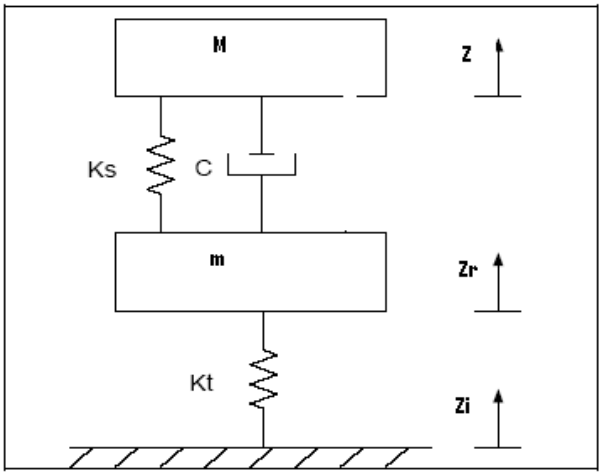

Figure 3-1: A physical model of quarter car model

The governing differential equations of this quarter car model are given as:

$$Md^2Z/dt^2 + Ks(Z - Zr) + C(dZ/dt - dZr/dt) = 0$$
$$md^2Zr/dt^2 + (Ks + Kt)Zr + C(dZr/dt) - KsZ - C(dZ/dt) - Kt(Zi/dt) = 0$$

Using these differential equations, a state space model is generated in MATLAB.The result of the simulation of this model by a ramp displacement input is shown in Fig 3-2:

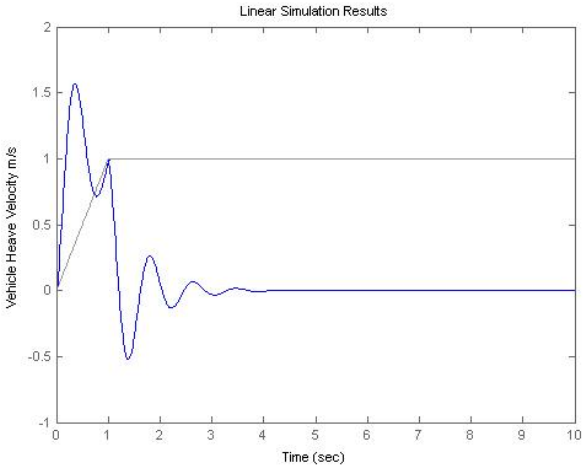

Figure 3-2: Output from state space model of quarter car model showing sprung mass velocity

In the Fig 3-2, the output is the velocity of the sprung mass. The bond graph model of the quarter car suspension is shown in Fig 3-3:

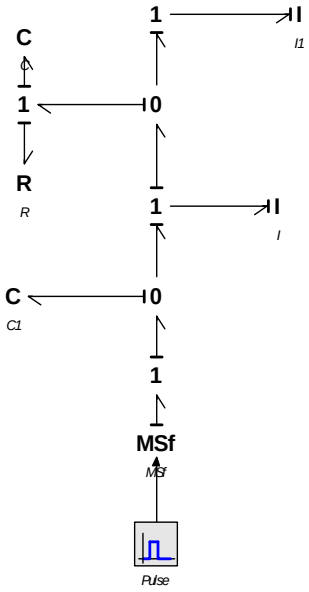

Figure 3-3: Bond graph model of quarter car suspension

This working of this bond graph model can be explained in a step by step manner:

1. The pulse signal goes to MSf or modulated flow variable which provides a flow input of type pulse for duration of 1 second to the first C element. This C element is a representation of the tire of the vehicle. The C is a compliance of tire and must be inverse of tire stiffness. According to the preferred causality on C element, a part of input velocity is taken up by the C element. The C element gives back the information about effort or force according to the constitutive equation of C element as explained in the previous chapter.

2. The effort from C element goes to the I or inertia element, which represents the tire mass. According to preferred causality the I element takes the information of flow and returns the information about flow. The C and I element together represent the tire.

3. The flow from I go to the C and R elements, the same flow information is received by these two elements. Both C and R elements return effort information. The constitutive equation for the R element is:

4. The two efforts are summed at the zero element and the resulting effort information goes to the second I element, which represents the vehicle body mass. The flow information returned by the I element is the response velocity of the vehicle body.

This model is simulated by providing it with a pulse velocity input which is equivalent to the ramp displacement input used in the simulation of quarter car state space model. The result of the simulation in 20Sim modeling software is shown in Fig 3-4

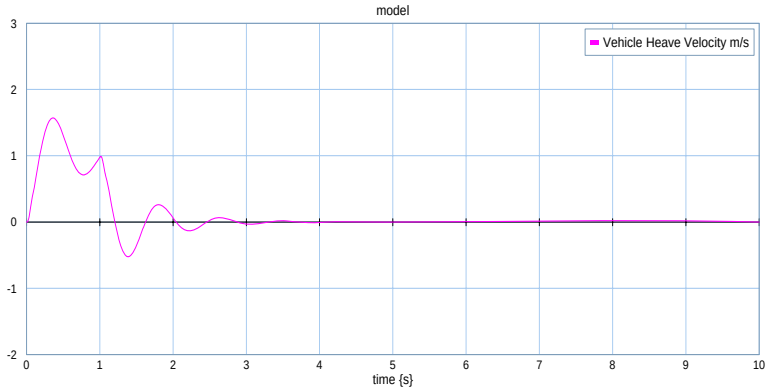

Figure 3-4: Output of bond graph quarter car model showing vehicle body velocity

It is seen that the velocity of the sprung mass is same in both cases. Thus the equivalence of the two models is established.

3.2 Half Car Suspension Model

A half car model also known as a bicycle car model is a logical extension to the quarter car model in that it includes the pitch motion of the vehicle in addition to the bounce motion. A physical half car suspension model is shown in the Fig 3-5:

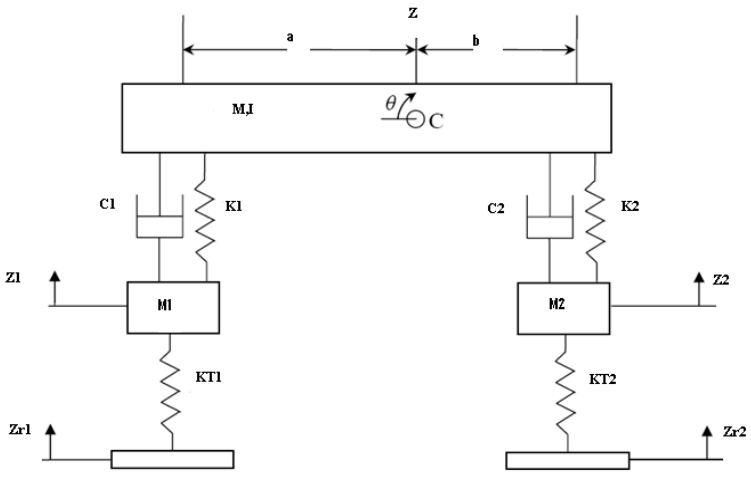

Figure 3-5:A physical model of half car suspension

This model has 4 degrees of freedom. The governing differential equations of this model are written as:

$$Md^2Z/dt^2 + K1(Z - a\theta - Z1) + C1(dZ/dt - ad\theta/dt - dZ1/dt) + K2(Z + b\theta - Z2) + C2(dZ/dt + bd\theta/dt - dZ2/dt) = 0$$

$$M1d^2Z1/dt^2 + (K1 + KT1)Z1 + C1dZ1/dt - K1(Z - a\theta - Z1) - C1(dZ/dt - a(d\theta/dt) - dZ1/dt) - KT1Zi1 = 0$$

$$M2d^2Z2/dt^2 + (K2 + KT2)Z2 + C2dZ2/dt - K2(Z + b\theta - Z2) - C2(dZ/dt + b(d\theta/dt) - dZ2/dt) - KT2Zi2 = 0$$

$$Id^2\theta/dt^2 = a\{K1(Z - a\theta - Z1) + C1(dZ/dt - ad\theta/dt - dZ1/dt)\} - b\{K2(Z + b\theta - Z2) + C2(dZ/dt + bd\theta/dt - dZ2/dt)\}$$

It is seen that the equations of motion now become complex since equations describing the pitch motion have to be included as well. Just like the case of quarter car model a state space model is generated from these equations in and simulated in MATLAB.

The same model is developed using bond graph method in 20Sim.It is shown in Fig 3-6:

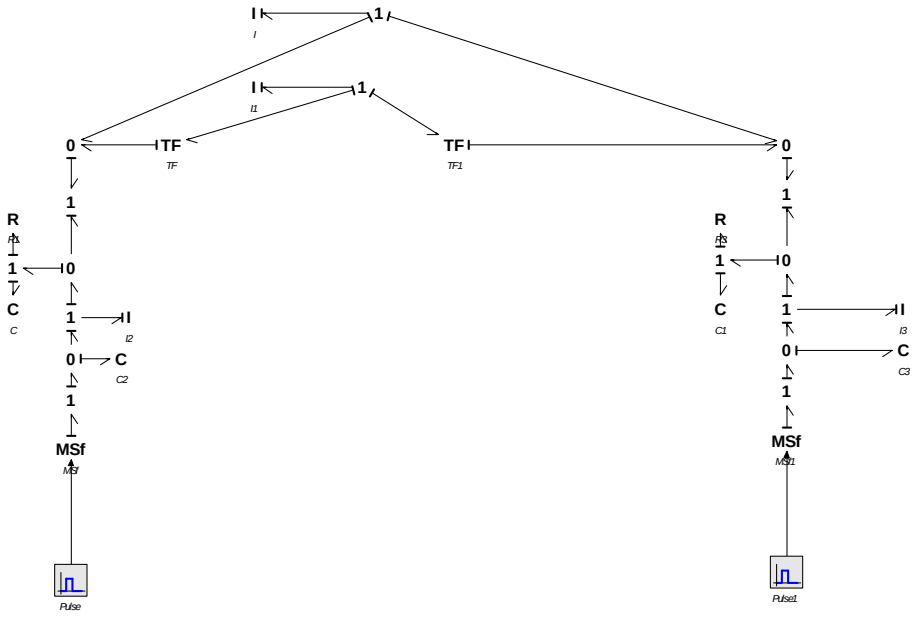

Figure 3-6: Bond graph model of half car suspension

When compared with quarter car bond graph model, it can be inferred that the half car bond graph model is composed of two quarter car models. However, some explanation is needed to fully understand the working of this model. As was done in the case of quarter car model, the working of half car model is explained in a step by step manner:

1. The model is similar to the quarter car model up to R and C elements connected to a common 1 element.

2. The effort information from the R and C elements connected to the common 1 element is divided into two forces at the zero elements (top most zero elements in the diagram).

3. One part of force goes to the I element representing vehicle mass, while the other part gets converted into a moment after passing through transformer element TF, and goes to the second I element representing the moment of inertia for pitch of vehicle body. The vehicle mass thus gives the information about the vehicle body linear velocity and the pitch moment of inertia gives the information about the angular velocity of the vehicle.

4. The above process occurs on two suspensions. The same input acts on the two suspensions; however, based on the vehicle speed and the separation between two suspensions the input will be delayed for the rear suspension by a time delay.

5. The suspension which receives the input pulse1 is the rear suspension and the it's transformation (TF1) value is set to be positive so that it produces positive moment and positive angular velocity, while TF is set at negative value so that we get negative moment and negative angular velocity from the front suspension.

The bond graph model is simulated for the same input as given to the analytical model. The input is the pulse velocity of amplitude 1m/s which corresponds to a ramp input of 1m from 1s to 2s.The input is applied to the rear suspension (shown as pulse1 in the model). The results of simulation are shown in Fig 3-7:

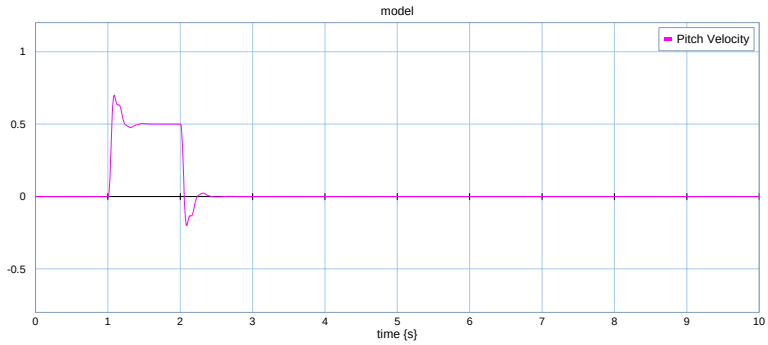

Figure 3-7: Output from bond graph model of half car suspension showing vehicle pitch velocity

3.3 Full Car Suspension Model

A full car suspension model includes roll, pitch and bounce motions of the vehicle body. Thus for full car suspension model the degrees of freedom increase to 7.A full car suspension model is shown in Fig 3-8:

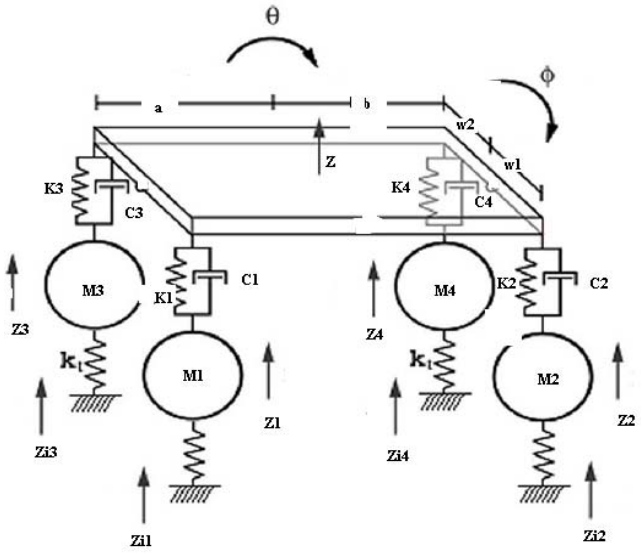

Figure 3-8: A physical model of full car suspension

The differential equations describing the dynamics of the full car suspension are written as:

$$
\begin{aligned}
&Md^2Z/dt^2 - KpZs - CpdZs/dt + K1(Z - a\theta - w1\phi - Z4) + C1(dZ/dt - ad\theta/dt - w1d\phi/dt - dZ4/dt)\\
&+ K2(Z + b\theta - w1\phi - Z2) + C2(dZ/dt + bd\theta/dt - w1d\phi/dt - dZ2/dt)\\
&+ K3(Z - a\theta + w2\phi - Z3) + C3(dZ/dt - ad\theta/dt + w2d\phi/dt - dZ3/dt)\\
&+ K4(Z + b\theta + w2\phi - Z4) + C4(dZ/dt - bd\theta/dt + w2d\phi/dt - dZ4/dt)\\
&+ KpZ + CpdZ/dt + Kpxp\theta + Cpxpd\theta/dt\\
&- Kpyp\phi - Cypyd\phi/dt = 0
\end{aligned}
$$

$$
\begin{aligned}
&M1d^2Z1/dt^2 + (K1 + Kt1)(Z1) + C1dZ1/dt - K1(Z - a\theta - w1\phi - Z1) - C1(dZ/dt - ad\theta/dt - w1d\phi/dt - dZ1/dt) - Kt1Zi1 = 0\\
&M2d^2Z2/dt^2 + (K2 + Kt2)(Z2) + C2dZ2/dt - K2(Z + b\theta - w1\phi - Z2) - C2(dZ/dt + bd\theta/dt - w1d\phi/dt - dZ2/dt) - Kt2Zi2 = 0\\
&M3d^2Z3/dt^2 + (K3 + Kt3)(Z3) + C3dZ3/dt - K3(Z - a\theta + w2\phi - Z3) - C3(dZ/dt - ad\theta/dt + w2d\phi/dt - dZ3/dt) - Kt3Zi3 = 0\\
&M4d^2Z4/dt^2 + (K4 + Kt4)(Z4) + C4dZ4/dt - K4(Z + b\theta + w2\phi - Z4) - C4(dZ/dt + bd\theta/dt + w2d\phi/dt - dZ4/dt) = 0
\end{aligned}
$$

$$
\begin{aligned}
&Id^2\theta/dt^2 =\\
&xpKpZs + xpCpdZs/dt + a\{K1(Z - a\theta - w1\phi - Z1) + C1(dZ/dt - ad\theta/dt - w1d\phi/dt - dZ1/dt) +\\
&K3(Z - a\theta + w2\phi - Z4) + C3(dZ/dt - ad\theta/dt + w2d\phi/dt - dZ4/dt)\} +
\end{aligned}
$$

$$-b\{K2(Z+b\theta-w1\phi-Z2)+C2(dZ/dt+bd\theta/dt-w1d\phi/dt-dZ2/dt)+$$
$$K4(Z+b\theta+w2\phi-Z3)+C4(dZ/dt+bd\theta/dt+w3d\phi/dt-dZ3/dt)\}$$

$$Jd^2\phi/dt^2 = ypKpZs+ypCpdZs/dt-w1\{K1(Z-a\theta-w1\phi-Z1)+C1(dZ/dt-ad\theta/dt-w1d\phi/dt-dZ1/dt)+$$
$$K2(Z+b\theta-w1\phi-Z2)+C2(dZ/dt+bd\theta/dt-w1d\phi/dt-dZ2/dt)\}+$$
$$+w2\{K4(Z+b\theta+w2\phi-Z4)+C4(dZ/dt+bd\theta/dt+w2d\phi/dt-dZ4/dt)+$$
$$K3(Z-a\theta+w2\phi-Z3)+C3(dZ/dt-ad\theta/dt+w2d\phi/dt-dZ3/dt)\}$$

The values of various parameters associated with the vehicle suspension are given in the table 3-1.

Table 3-1: Parameter values for full car suspension

Parameters	Values
Front Right and Left Tire Stiffness (k_{t1}, k_{t2})	200000 N/m
Rare Right and Left Tire Stiffness (k_{t3}, k_{t4})	200000 N/m
Front Right and Left Suspension Stiffness (k_{s1}, k_{s2})	32000 N/m
Rare Right and Left Suspension Stiffness(k_{s3}, k_{s4})	40000 N/m
Passenger Seat Stiffness (k_{s5})	90000N/m
Passenger Seat Damping (c_{s5})	2500Ns/m
Front Right and Left Suspension Damping (c_{s1}, c_{s2})	2500 Ns/m
Rare Right and Left Suspension Damping(c_{s3}, c_{s4})	2500
Front Right and Left Tire Masses (m_{u1}, m_{u2})	60 kg
Rare Right and Left Tire Masses (m_{u3}, m_{u4})	85 kg
Mass of Vehicle Body (*M*)	1100 kg
Linear Distance of Front Axle from COG (a)	1.2 m
Linear Distance of Rare Axle from COG (b)	1.4 m
Linear Distance of left body side bar to COG (d)	1 m
Linear Distance of Right body side bar to COG (c)	0.5 m
Linear Distance of Passenger seat from side bar (f)	0.375m
Linear Distance of Passenger seat from front bar (e)	0.25 m

From these equations a state space model is developed and simulation is performed in MATLAB.The results of the simulation are shown in Fig 3-9:

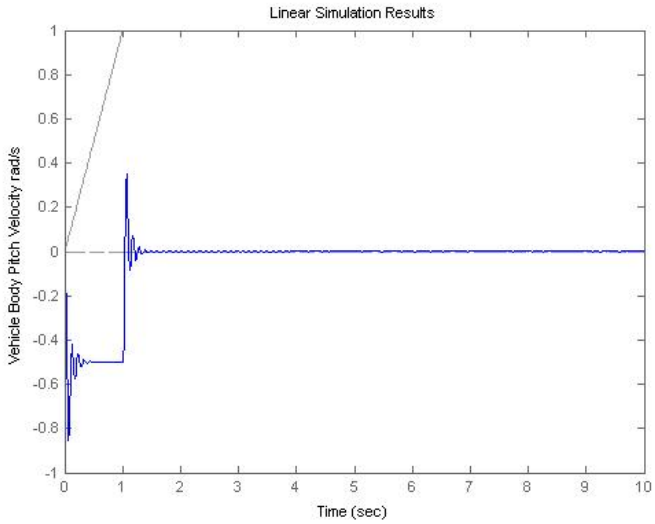

Figure 3-9: Output of state space model of full car suspension showing vehicle pitch velocity

The parameter values used for the simulation are those used by. These values are given in table.

The bond graph model of the full car suspension generated in 20Sim is shown in Fig 3-10:

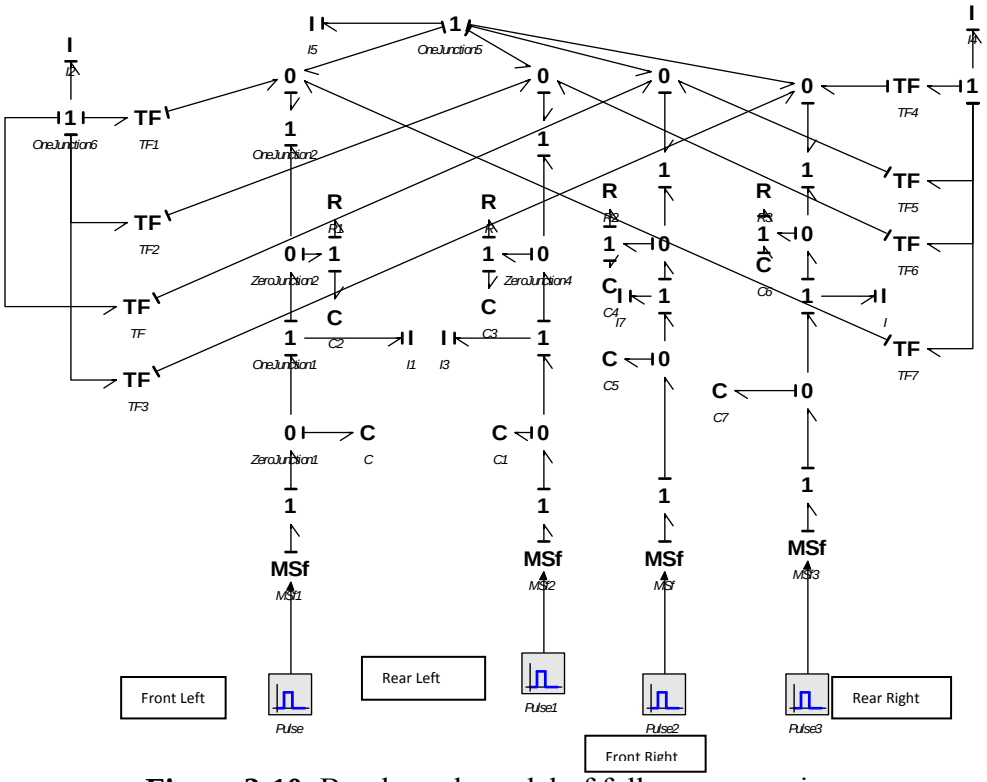

Figure 3-10: Bond graph model of full car suspension

The working of this model is explained in a step by step manner:

1. This model has four suspensions. The inputs pulse, pulse1, pulse2 and pulse3 go to suspensions 1, 2, 3 and 4 respectively.

2. Consider suspension1.The effort from R and C elements connected to the common 1 element, distribute into three parts at the 0 element placed at the top of this suspension. Recall half car model where the same effort was distributed into two parts, one got converted into moment and the other acted on the vehicle mass.In a full car model since rolling motion of vehicle also occurs hence a third moment is needed to cause rolling motion. Thus of the three parts of effort, one acts on the vehicle mass, one gets converted into pitching moment and one gets converted into rolling moment. The pitching moment acts on the pitch moment of inertia and the rolling moment acts on roll moment of inertia. Also two transformers are present per suspension

3. Same case occurs for the other three suspensions. This makes total number of transformers equal to eight. Four convert the efforts to corresponding pitching moments and four to rolling moments.

4. Suspension1 and suspension3 form the front suspensions while suspension2 and suspension4 form rear suspension. According to the convention used front suspension produce negative pitching moments and the rear suspensions produce positive pitching moments. Also suspensions 1 and 3 produce positive rolling moments and suspensions 2 and 4 produce negative rolling moments.

The results of simulation are shown in the Fig 3-11, for the same kind of input as given to the state space MATLAB model.

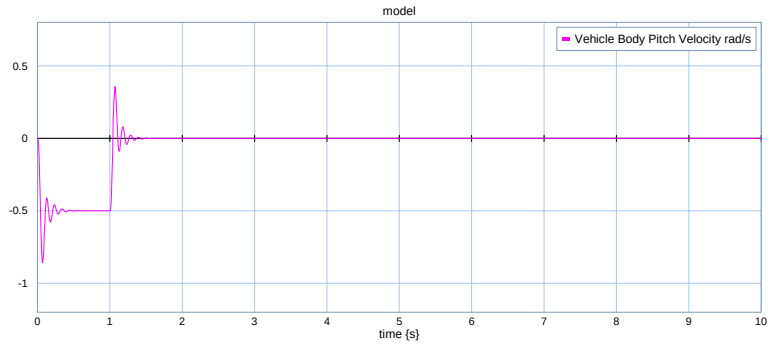

Figure 3-11: Output of graph model of full car suspension showing vehicle pitch velocity

As the results of two simulations match with, hence it is deduced that two models are equivalent.

3.4 Validation of Full Car Suspension Model

The full car suspension model is confirmed by comparing it's results with a full car suspension model developed in reference [10].The model available in literature has 8 degrees of freedom as this model also includes passenger seat. The physical model is shown in Fig 3-12.

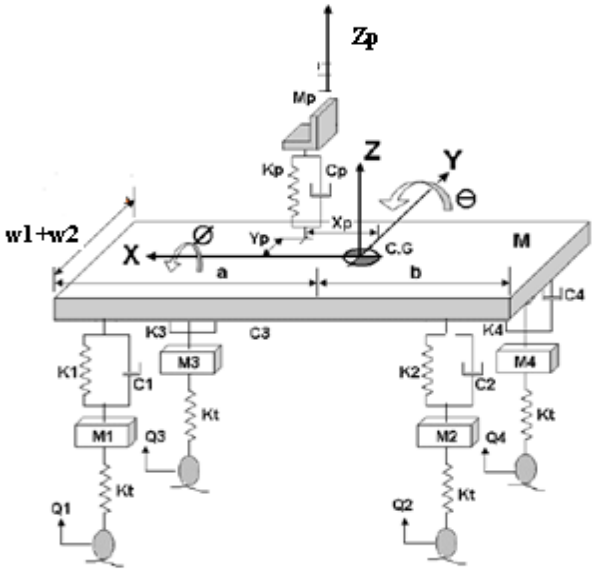

Figure 3-12: Physical model of full car suspension showing passenger seat

Because of the inclusion of passenger seat; the governing differential equations are slightly modified. The equations are given on the next page. A state space model is generated

from these equations. At this point it is pertinent to mention that the state space model generated for the 7 degrees of freedom full car suspension in section 3.3 is similar to the state space model for 8 dof suspension model with the only difference that for 7 dof state space model the passenger seat compliance and damping and it's distances from CG of vehicle body are taken equal to zero.

$$Mpd^2Zs/dt^2 + KpZs + CpdZs/dt - KpZ - CpdZ/dt - Kpxp\theta - xpCpd\theta/dt + Kpyp\phi + Cpypd\phi/dt = 0$$

$$\begin{aligned}
&Md^2Z/dt^2 - KpZs - CpdZs/dt + K1(Z - a\theta - w1\phi - Z4) + C1(dZ/dt - ad\theta/dt - w1d\phi/dt - dZ4/dt)\\
&+ K2(Z + b\theta - w1\phi - Z2) + C2(dZ/dt + bd\theta/dt - w1d\phi/dt - dZ2/dt)\\
&+ K3(Z - a\theta + w2\phi - Z3) + C3(dZ/dt - ad\theta/dt + w2d\phi/dt - dZ3/dt)\\
&+ K4(Z + b\theta + w2\phi - Z4) + C4(dZ/dt - bd\theta/dt + w2d\phi/dt - dZ4/dt)\\
&+ KpZ + CpdZ/dt + Kpxp\theta + Cpxpd\theta/dt\\
&- Kpyp\phi - Cpypd\phi/dt = 0
\end{aligned}$$

$$\begin{aligned}
&M1d^2Z1/dt^2 + (K1 + Kt1)(Z1) + C1dZ1/dt - K1(Z - a\theta - w1\phi - Z1) - C1(dZ/dt - ad\theta/dt - w1d\phi/dt - dZ1/dt) - Kt1Q1 = 0\\
&M2d^2Z2/dt^2 + (K2 + Kt2)(Z2) + C2dZ2/dt - K2(Z + b\theta - w1\phi - Z2) - C2(dZ/dt + bd\theta/dt - w1d\phi/dt - dZ2/dt) - Kt2Q2 = 0\\
&M3d^2Z3/dt^2 + (K3 + Kt3)(Z3) + C3dZ3/dt - K3(Z - a\theta + w2\phi - Z3) - C3(dZ/dt - ad\theta/dt + w2d\phi/dt - dZ3/dt) - KtQ3 = 0\\
&M4d^2Z4/dt^2 + (K4 + Kt4)(Z4) + C4dZ4/dt - K4(Z + b\theta + w2\phi - Z4) - C4(dZ/dt + bd\theta/dt + w2d\phi/dt - dZ4/dt) - KtQ4 = 0
\end{aligned}$$

$$\begin{aligned}
&Id^2\theta/dt^2 = xpKpZs + xpCpdZs/dt + a\{K1(Z - a\theta - w1\phi - Z1) + C1(dZ/dt - ad\theta/dt - w1d\phi/dt - dZ1/dt)\\
&+ K3(Z - a\theta + w2\phi - Z4) + C3(dZ/dt - ad\theta/dt + w2d\phi/dt - dZ4/dt)\} +\\
&- b\{K2(Z + b\theta - w1\phi - Z2) + C2(dZ/dt + bd\theta/dt - w1d\phi/dt - dZ2/dt) +\\
&K4(Z + b\theta + w2\phi - Z3) + C4(dZ/dt + bd\theta/dt + w3d\phi/dt - dZ3/dt)\}\\
&+ xpKpZ + xpCpdZ/dt - xp^2Kp\theta - xp^2Cpd\theta/dt + xpypKp\phi + xpypCpd\phi/dt
\end{aligned}$$

$$\begin{aligned}
&Jd^2\phi/dt^2 = ypKpZs + ypCpdZs/dt - w1\{K1(Z - a\theta - w1\phi - Z1) + C1(dZ/dt - ad\theta/dt - w1d\phi/dt - dZ1/dt) +\\
&K2(Z + b\theta - w1\phi - Z2) + C2(dZ/dt + bd\theta/dt - w1d\phi/dt - dZ2/dt)\} +\\
&+ w2\{K4(Z + b\theta + w2\phi - Z4) + C4(dZ/dt + bd\theta/dt + w2d\phi/dt - dZ4/dt) +\\
&K3(Z - a\theta + w2\phi - Z3) + C3(dZ/dt - ad\theta/dt + w2d\phi/dt - dZ3/dt)\} - KpypZ - CpypdZs/dt\\
&- ypxpKp\theta - ypxpCpd\theta/dt - yp^2Kp\phi - yp^2Cpd\phi/dt
\end{aligned}$$

The passenger seat is modeled as a mass ms attached to vehicle body at distances horizontal distances xp and yp from the center of gravity of the vehicle body. The displacement of the passenger seat is Zs.The inputs used are shown in the Fig 3-13:

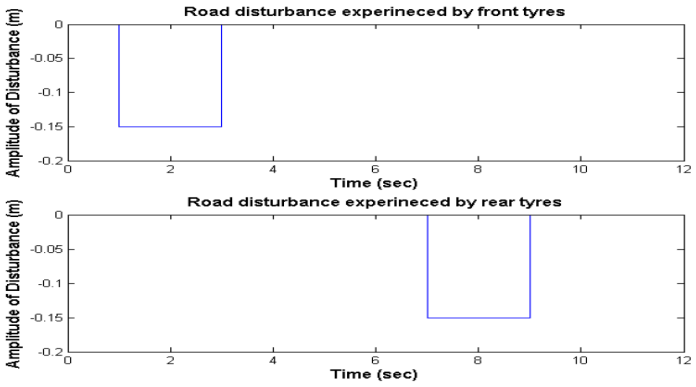

Figure 3-13: Inputs applied to full car suspension with passenger seat

The response of vehicle body heave motion and pitch motion as obtained in reference[10] are shown in Fig 3-14:

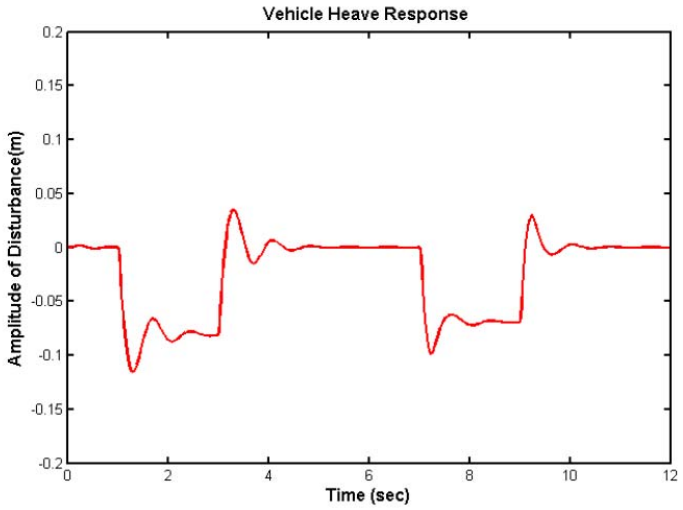

Figure 3-14: Vehicle body heave response

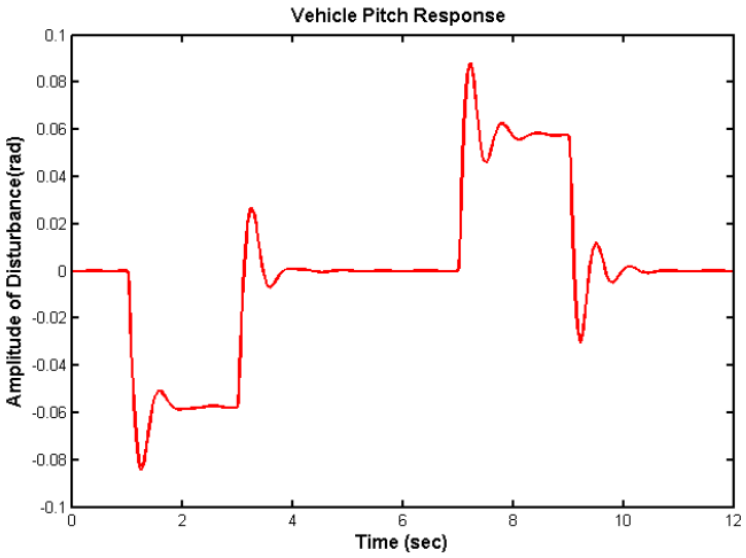

Figure 3-15: Vehicle body pitch response

Now the same parameters as used by are provided to the full car suspension state space model developed in section. The model is simulated for the same inputs as shown in Fig 3-12. The vehicle body pitch response and heave response are shown on Fig 3-16 and Fig 3-17 respectively.

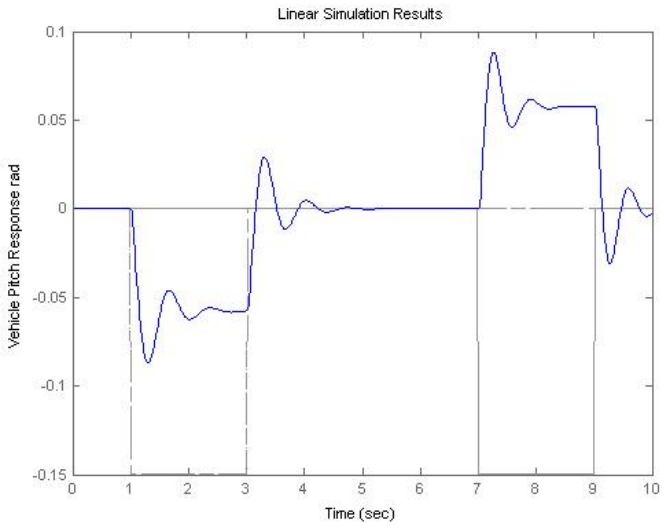

Figure 3-16: Output of state space model of full car suspension with passenger seat showing vehicle heave response

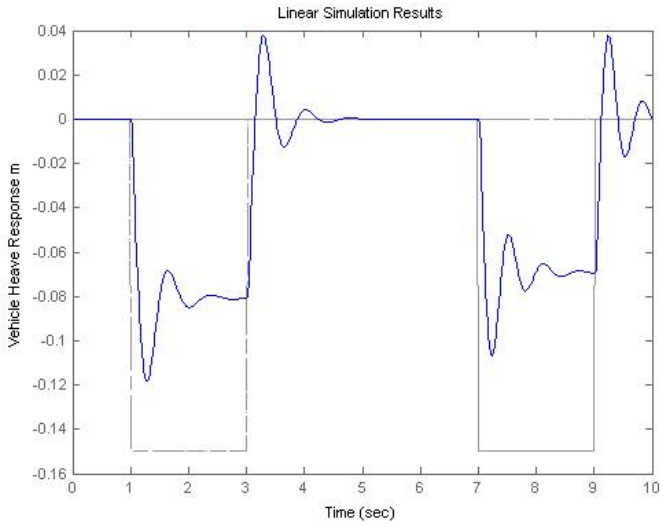

Figure 3-17: Output of state space model of full car suspension with passenger seat showing vehicle body heave response

It is seen that the outputs are the same for the literature model and the state space model developed in the present section. The current 8 dof vehicle suspension model is an extension to the 7 dof model developed in the previous section. Thus the validation of the 8dof model automatically validates the 7 dof vehicle suspension model.

3.5 Vector Bond Graph Model of Full Car Suspension

A vector bond graph differs from the 1D bond graph in that it carries a vector of power signal between various interconnected components of a system. In 1D bond graph the signal is a scalar. Thus the vector of power signal between various interconnected components carries x,y and z components of the power signal, similarly the response of the model can also be observed in terms of the x,y and z components of response. The significance of the vector bond graph arises from the fact that a 3D dynamic system like full car suspension exhibits motion in 3D.Thus the bounce motion may not be purely vertical but may have components in other directions as well. Thus with vector bond graphs it becomes possible to realize the behavior of dynamic system as close to real world as possible. The vector bond graph model of the full car suspension is shown in the Fig 3-18:

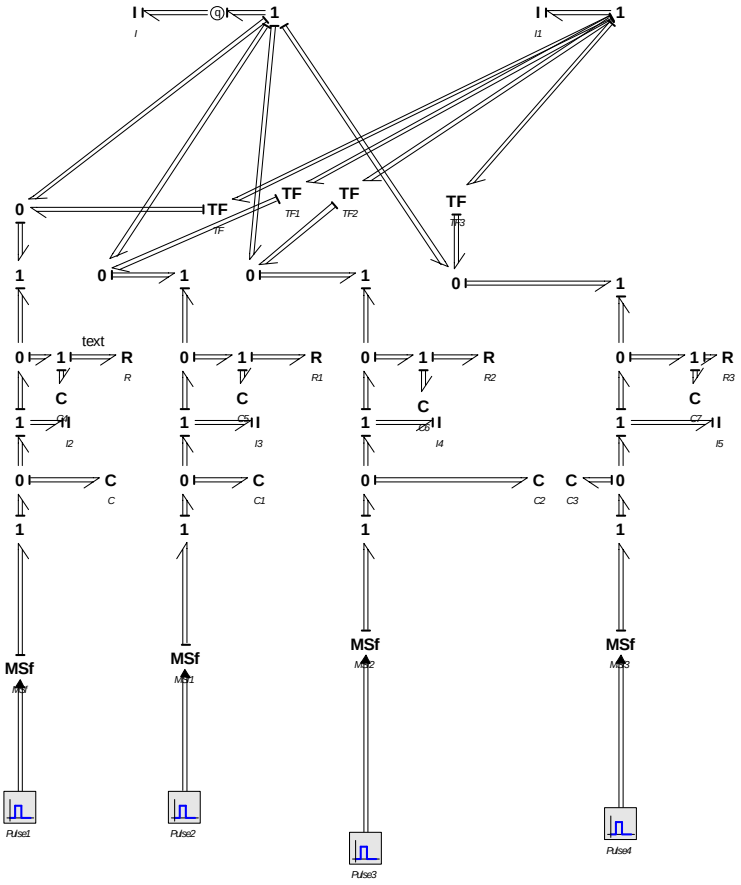

Figure 3-18: Vector bond graph model of full car suspension

The results of the simulation of the vector bond graph model of Fig for the same kind of inputs as that of the 1D bond graph model given in Fig is shown in Fig 3-19:

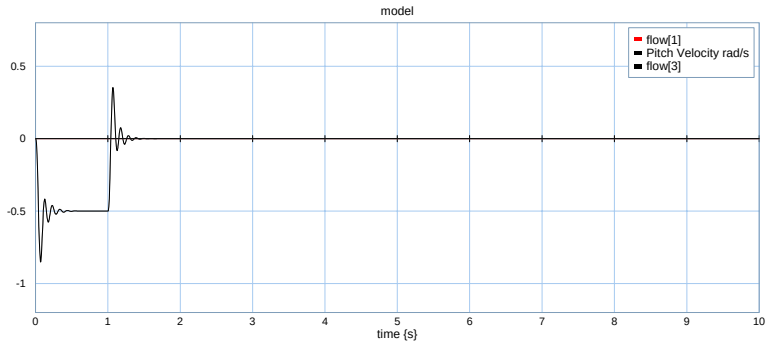

Figure 3-19: Output of vector bond graph model of full car suspension showing vehicle body pitch response

3.6 Full Car Vector Bond Graph Model with Mounted Component

The full car suspension model now needs to be modified to include a mounted component on the vehicle body. The component mounted is a thin steel plate attached to the vehicle body at four points. The purpose here is to show the transmissibility of road inputs to the component and the resulting effect on fatigue life. Thus it is just like another body mounted on the vehicle body. The vector bond graph of the vehicle with mounted component is shown in Fig 3-20:

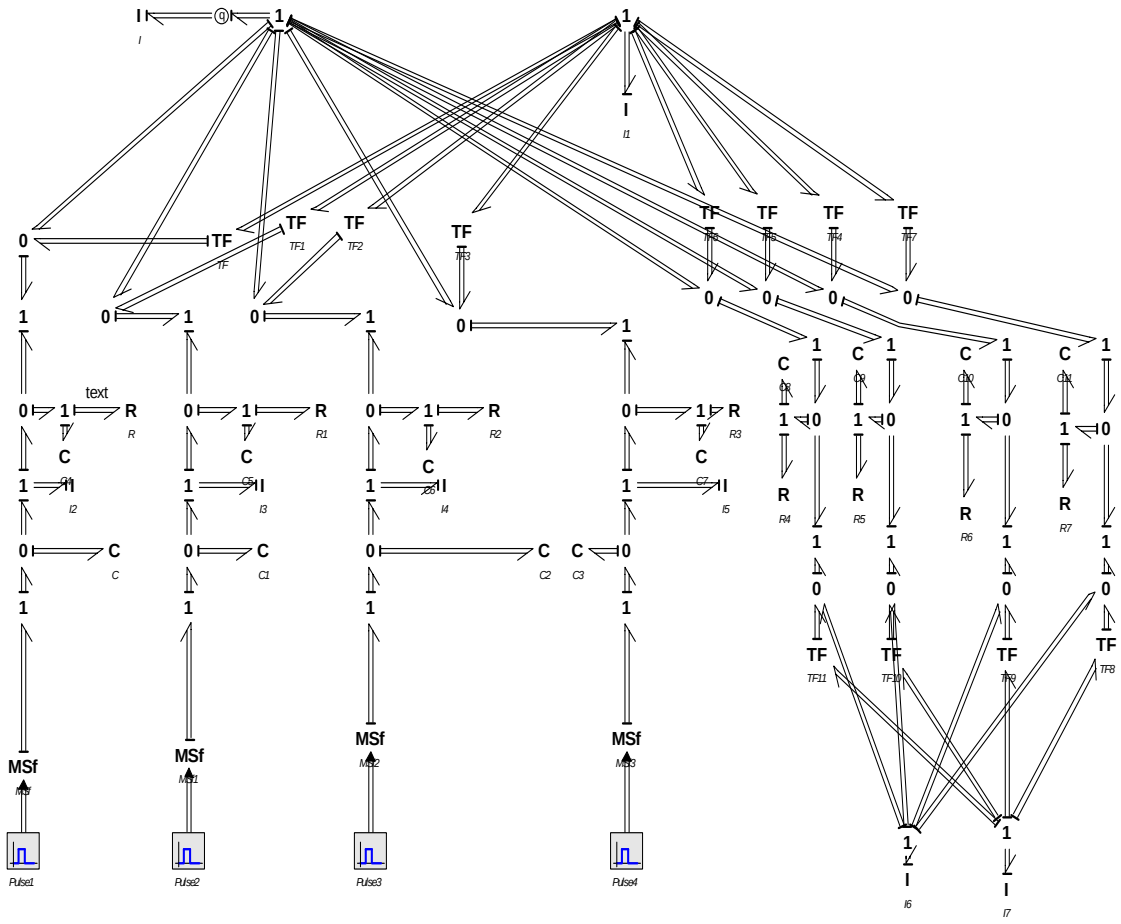

Figure 3-20: Vector bond graph model of full car suspension augmented to include mounted component

The CAD model of the mounted component is shown in Fig 3-21. The material of the plate is structural steel. The points of application of force are also shown.

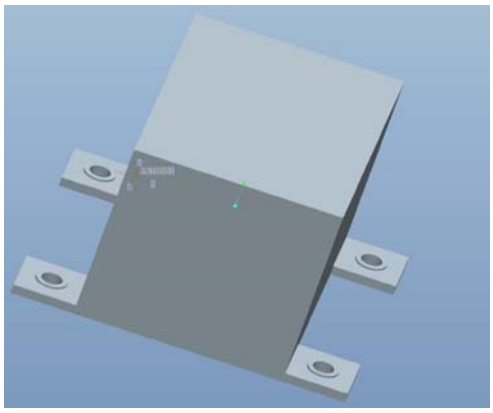

Figure 3-21: CAD model of mounted component

In the Fig 3-21, the points of attachment are the holes. One of the holes is shown by arrow. The component is bolted at these holes to the vehicle body. The slightly protruding surfaces around the holes are the areas over which the force of bolt head would act. Thus while carrying out the finite element analysis of the part; the load values from 20Sim would be transferred to these areas.

3.6.1 Use of Anti-Vibration Mounts

In the present study, the part attachment to the vehicle body has been made through anti vibration mounts, thus the vibration transmissibility to the attached part has been reduced. The anti-vibration mount performs the same function as that of a suspension system, thus mitigating the vibration levels reaching the component. The Fig 3-22 shows the way parts are attached using anti-vibration mounts.

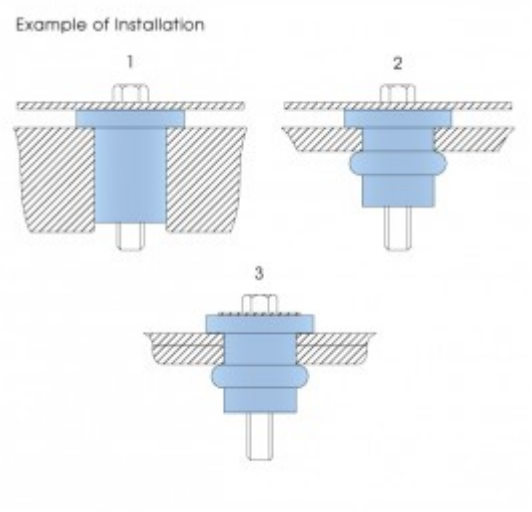

Figure 3-22: Part attachment using anti-vibration mounts

As is clear from the figure, an anti-vibration mount consists of a rubber pad and a bolt. Thus an anti-vibration mount can be modeled by a single spring element or stiffness; which itself is a linear combination of two spring elements or stiffnesses; one for the rubber pad, and one for the bolt. In other words, the combined stiffness of the two elements of the anti-vibration mount is simply the sum of the stiffnesses of the two elements. Also the resistance coefficients of the two elements are added to obtain combined resistance of anti-vibration mounts. We write:

$$R_{combined} = R_{pad} + R_{bolt} \tag{3.1}$$

$$K_{combined} = K_{pad} + K_{bolt} \tag{3.2}$$

3.6.2 Coordinate Transformation

The bond graph model of Fig 3-19 is a satisfactory representation of the vehicle suspension system as far as the angular displacements of the vehicle body arising from the roll, pitch and yaw motion of the vehicle body are small.Thus,the body attached coordinate system and the inertial coordinate system are reasonably the same. However, large angular displacements of the vehicle body arising from travel on rough road conditions etc demand the velocities, forces etc reaching the vehicle body from the suspension be represented in terms of their components in the body coordinate system. In the Fig 3-23, the same vector bond graph model is shown in modular form. The gtl block concerts the values to the local or body

coordinate system. The conversion process involves multiplying the variable by three matrices namely yaw, pitch and roll.

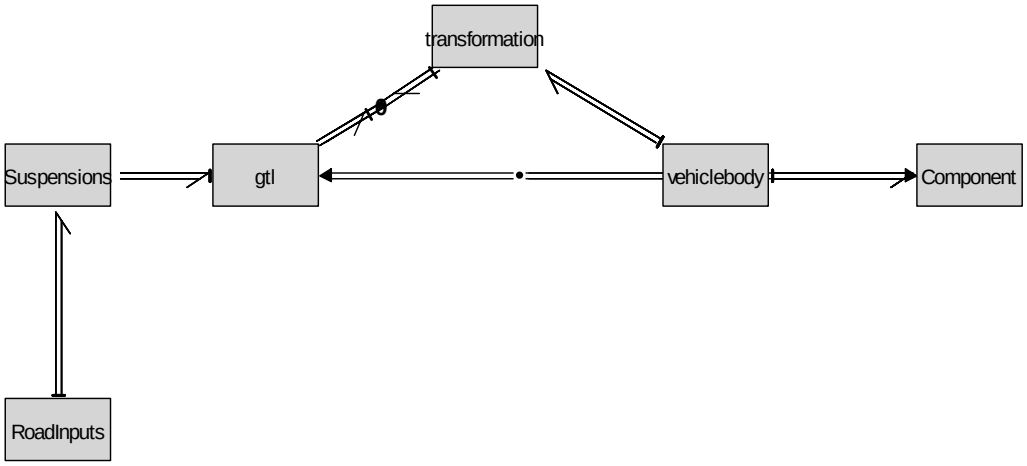

Figure 3-23: Modular form of vector bond graph model of full car suspension

The extended model of the gtl block is shown in Fig 3-24:

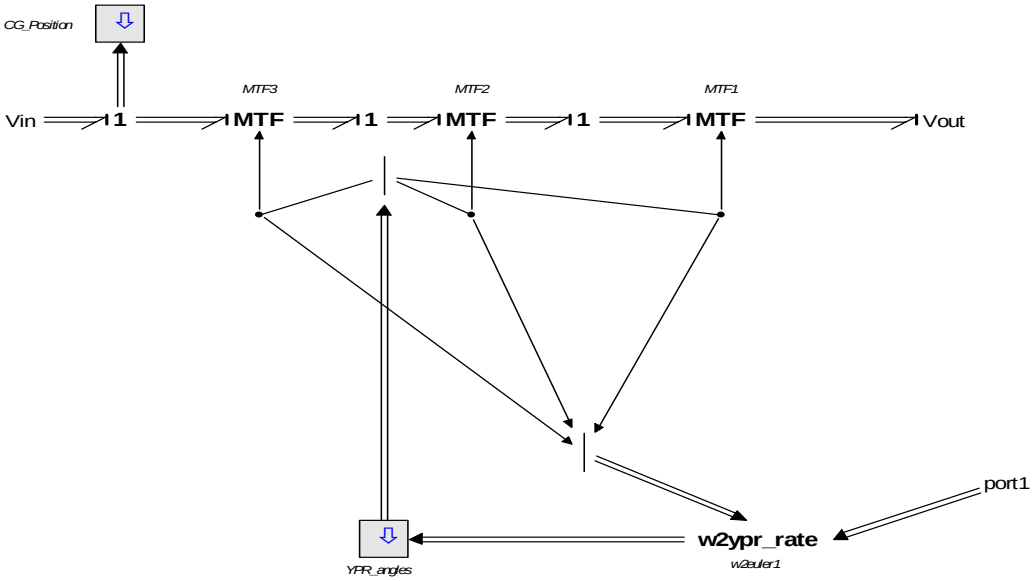

Figure 3-24: Extended model of gtl block

In the fig, Vin is the effort or force input signal, while each MTF block represents a conversion matrix. The force signal gets multiplied by three conversion matrices and gets converted to body coordinate system represented by Vout[11]

The conversion matrices used are for yaw, roll and pitch. The force signal gets multiplied successively by yaw, pitch and roll matrices respectively. This order of multiplication has been established by a method explained in .The body is initially at a position such that the body fitted coordinate system coincides with the global coordinate system. The body is assumed to undergo yaw, pitch and roll motions successively and the final coordinate system is then determined by the following equation:

$$\begin{aligned}\vec{x}_b &= R(\psi)R(\theta)R(\phi)\vec{x} \\ &= \begin{bmatrix} c\theta c\phi & c\theta s\phi & -s\theta \\ -c\psi s\phi + s\psi s\theta c\phi & c\psi c\phi + s\psi s\theta s\phi & s\psi c\theta \\ s\psi s\phi + c\psi s\theta c\phi & -s\psi c\phi + c\psi s\theta s\phi & c\psi c\theta \end{bmatrix} \vec{x} \\ &= R(\phi,\theta,\psi)\vec{x}.\end{aligned}$$

Here $R(\psi)$, $R(\theta)$, and $R(\varphi)$ represent transformation matrices for roll, pitch and yaw respectively.If we go step by step, let x_b^0 be the inertial frame, and it undergoes rotation through an angle φ about the z axis, then the transformed frame x_b^1 is given by:

$$\vec{x}_b^{\,1} = \begin{bmatrix} \cos\phi & \sin\phi & 0 \\ -\sin\phi & \cos\phi & 0 \\ 0 & 0 & 1 \end{bmatrix} \vec{x}_b^{\,0} = R(\phi)\vec{x}_b^{\,0}.$$

Similarly the transformed frame x_b^1 now undergoes rotation through an angle θ about y axis, the transformed frame x_b^2 is given by:

$$\vec{x}_b^{\,2} = \begin{bmatrix} \cos\theta & 0 & -\sin\theta \\ 0 & 1 & 0 \\ \sin\theta & 0 & \cos\theta \end{bmatrix} \vec{x}_b^{\,1} = R(\theta)\vec{x}_b^{\,1}.$$

Finally the frame x_b^2 undergoes rotation through an angle ψ about x axis, the final frame x_b^2 is given by:

$$\vec{x}_b^3 = \begin{bmatrix} 1 & 0 & 0 \\ 0 & \cos\psi & \sin\psi \\ 0 & -\sin\psi & \cos\psi \end{bmatrix} \vec{x}_b^2 = R(\psi)\vec{x}_b^2.$$

The transformation to body attached coordinate system is now complete with x_b^3 representing the transformed coordinate system.

The vector bond graph shown in Fig allows the determination of response of any point on the vehicle body, as well as the response of the attached component. Both velocity response and force response values can be used to determine the dynamic stresses generated in the component.

From this point onwards the actual vehicle parameter values will be used to simulate the bond graph models. The parameter values are those used by .These parameter values are given in table 3-2.

Table 3-2: Parameter values for full car suspension bond graph model

Parameter	Value
K1,K3	36297 N/m
K2,K4	19620 N/m
C1,C3	3924 Ns/m
C2,C4	2943 Ns/m
M	1136 kg
M1,M3	63 kg
M2,M4	60 kg
Ixx	460 kgm^2
Iyy	2160 kgm^2

CHAPTER 4: GENERATION OF TIME BASED RANDOM ROAD INPUT

In the previous chapter, vector bond graph model of full car suspension was generated. The present chapter deals with generation of random road profile which will be used as input to the bond graph model. The procedure for generation of various road profiles as described in reference [12] is followed.

4.1 Why Random Road Profile

All road profiles whether are random in nature. To study the suspension performance in actual conditions, the road should be modeled as a stochastic process. While simple road profiles such as sine wave or step can be used to compare the performance of various suspensions, they cannot be used to study the suspension behavior in actual operating conditions. A random process is one in which the exact value of the signal at a future time instant cannot be described by a functional relationship. However, if sufficient knowledge of the mechanism producing random data is available then it is possible to describe the process with exact mathematical relationships.

A random road profile is described in terms of power spectral density (PSD) function. Power spectral density of the road is measured by digital spectral density analyzers and is used to classify various types of road surfaces.

4.2 Ergodig Road Profile

Consider Fig on next page:

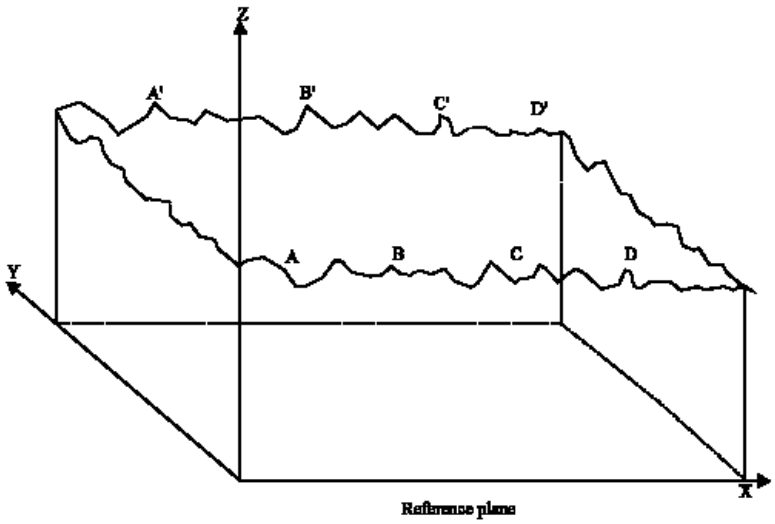

Figure 4-1: Ergodic road profile

if the profile in A-D and A'-D' in parallel planes would be the same, the profile is ergodic. This would be the most ideal situation and in this case, by developing a method to produce a part of a profile, it can be extended to produce a 2D or 3D model of the whole path.

4.3 Classification of Road Surface

The international standardization organization (ISO) has proposed road roughness classification based on PSD of road surface profiles. The mathematical relationship between the PSD and spatial frequency is written as:

$$G_u(\Omega) = C_{sp}.\Omega^{-N} \tag{4.1}$$

The values of C_{sp} and N for various types of roads are shown in the table.

The spatial frequency Ω is of the road profile when plotted as a function of distance. Thus the PSD represented by equation is in the spatial domain.

4.4 PSD to time Domain Conversion of Road Input Profile

Random road profile generation involves generation of discrete Fourier transform (DFT) with desired PSD.Inverse Fourier transform of the DFT gives the road profile which is a time signal.

The Fourier transform $u(f)$ is a complex number given as:

$$u(fk) = R(fk) + I(fk) \tag{4.2}$$

Here $u(fk)$ is the discrete Fourier transform of the road profile $u(t)$.The objective then becomes to generate the real part $R(fk)$ and the imaginary part $I(fk)$ of the discrete Fourier transform $u(fk)$ and adding them to get $u(fk)$.

The equations to find the $R(fk)$ & $I(fk)$ are given as:

$$R(fk) = \sqrt{G(fk)\frac{NH}{2}}.\cos(\theta) \tag{4.3}$$

$$I(fk) = \pm j.\sqrt{G(fk)\frac{NH}{2}}.\ \sin(\theta) \tag{4.4}$$

These values are discrete as these are generated at discrete frequency points. The values of θ varies from 0 to 2Π.The PSD in the frequency domain is given by the relation:

$$Gu(fk) = \frac{G_u(\Omega)}{V.(\frac{f}{V})^N} \tag{4.5}$$

Ω is the spatial frequency, while f is the temporal frequency.Once we have the values of $u(fk)$, we take it's discrete Fourier transform to find $u(t)$.

In this study ergodic profile has been used to simulate the vehicle response. This means that the left and the right wheels of the vehicle experience same type of road excitations. Thus we shall apply the signal u(t) as input to both the left and right suspensions of the vehicle model. The signal u(t) reaches the rear left and right suspensions by a time delay. This time delay is calculated by dividing the length of vehicle by the velocity of vehicle travel on the road:

$$t = \frac{L}{V} = \frac{2.8}{16.66} = 0.1680S \tag{4.6}$$

The road profile generated for a vehicle travelling at 60km/h is shown in Fig 4-2:

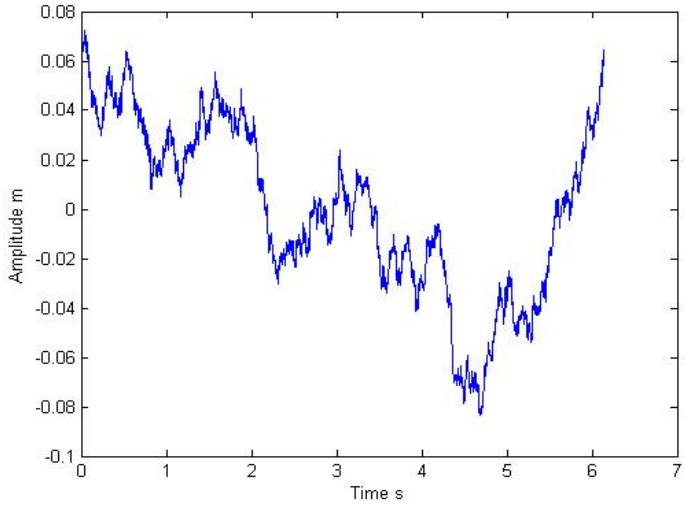

Figure 4-2: Temporal road profile of rough road

CHAPTER 5: FATIGUE LIFE ESTIMATION

In this chapter, fatigue life estimation of the component mount will be carried out. Now that road profile is available, we can provide this road profile as input to vector bond graph model of the vehicle. The velocities of excitation to the component are the linear and angular velocity values of the vehicle body to which component is attached at four mounting points. Before moving toward detailed discussion regarding fatigue behavior of the component, basics of fatigue analysis due to random vibrations will be explained.

5.1 Fatigue

Fatigue is the process of progressive localized permanent structural change occurring in a material subjected to conditions that produce fluctuating stresses and strains at some point or points and that may culminate in cracks or complete fracture after a sufficient number of fluctuations. Fatigue life is divided into three stages: crack initiation, crack propagation and it's growth up to a critical length. Usually, crack initiation time is taken as the fatigue life of the component.

Fatigue occurs due to loads which are cyclic in nature. Such cyclic loads cause fracture of the component even if the stress amplitude is below the yield point of the material. Due to this rather unusual behavior, fatigue is the most important failure mode to be considered in the design of mechanical parts. The physical process of fatigue is described in Figure 5-1. Under the action of oscillatory tensile stresses of sufficient magnitude, a small crack will initiate at a point of the stress concentration. Once the crack is initiated, it will tend to grow in a direction orthogonal to the direction of the oscillatory tensile loads.

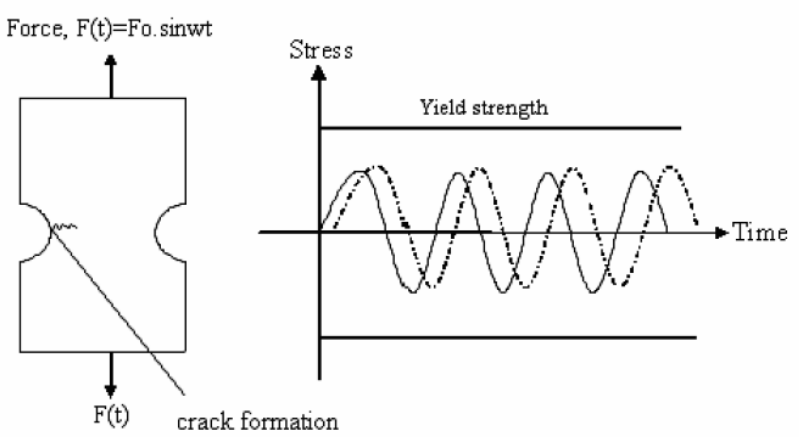

Figure 5-1: Uniform fluctuation stress and fatigue crack formation

If the cyclic loading is of uniform nature then it is possible to tell the number of cycles N, the component would endure before fatigue failure occurs simply by using the Wöhler S-N curve that is a plot of alternating stress, S, versus cycles to failure, N.

5.1 Fatigue due to Random Loads

Loading conditions in actual service of the part are far from uniform. Mechanical systems such as automobile suspension, aeronautical structures etc experience random loading during service and the fatigue life cannot be assessed merely by looking at the S-N curve of the material, as the stresses generated are also of random nature.

This limitation is addressed by using rainflow cycle counting method which counts the number of cycles of various amplitudes existing in a random time signal. When applied to the random stress data, cycles of various stress levels are counted by the algorithm. Once the stress cycles become available, Palmgren-Miner's rule of cumulative fatigue damage is applied to estimate the time to failure of part due to fatigue. The subsequent sections of this chapter describe in detail the process of fatigue life calculation of the component mounts due to random excitations on the vehicle body.

5.2 Mounting Locations of Component on Vehicle Body

The fatigue life of the component is calculated at four mounting locations on vehicle body. These mounting locations are as follows:

1. *Corner Mounting Location:* This mounting location is shown in Fig 5-2.Here the component is mounted at the front left corner of the vehicle, such that the front left corner of component and that of vehicle coincide.

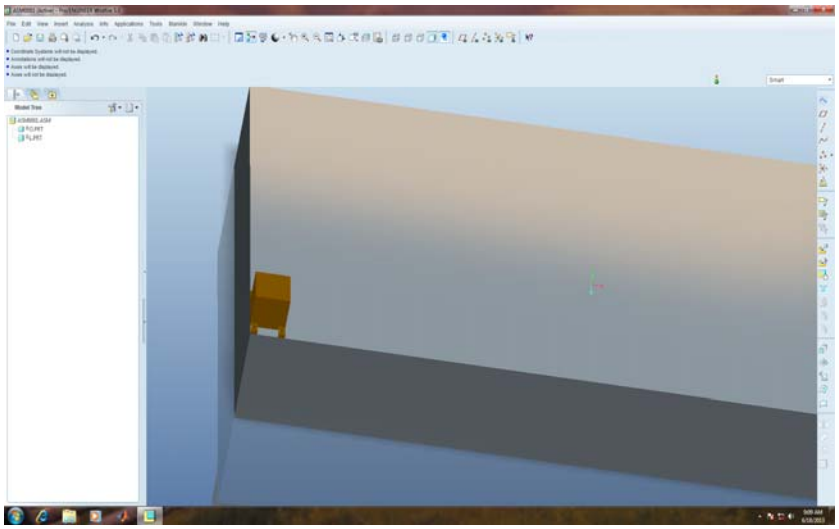

Figure 5-2: Corner Mounting Location

2. *Front Mounting Location:* This mounting location is shown in Fig 5-3.Here the component is mounted at the front side of the vehicle.

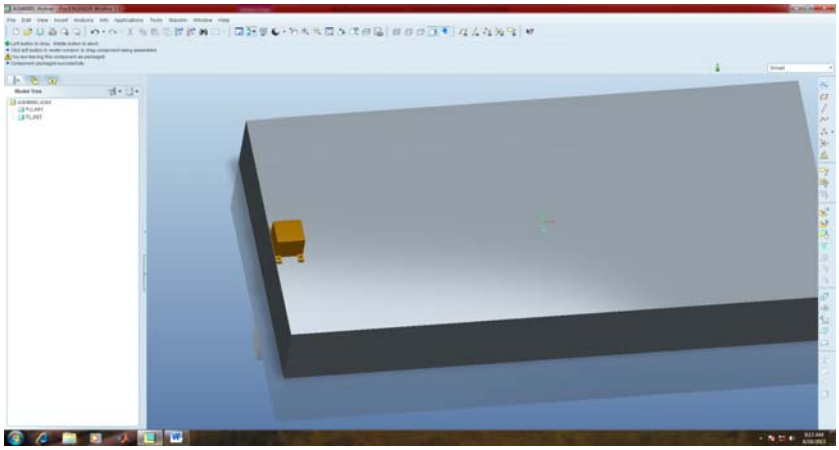

Figure 5-3: Front Mounting Location

3. *CG Mounting Location:* This mounting location is shown in Fig 5-4.Here the component is mounted at the CG of the vehicle body, such that the center of component and CG of vehicle body coincide.

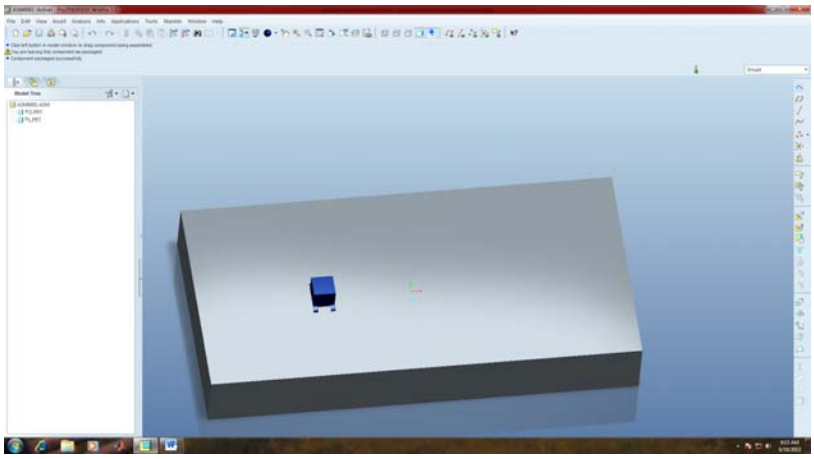

Figure 5-4: CG mounting Location

4. *Center Mounting Location:* This mounting location is shown in Fig 5-5.Here the component is mounted at the geometric center of the vehicle body, such that the center of component and that of vehicle body coincide.

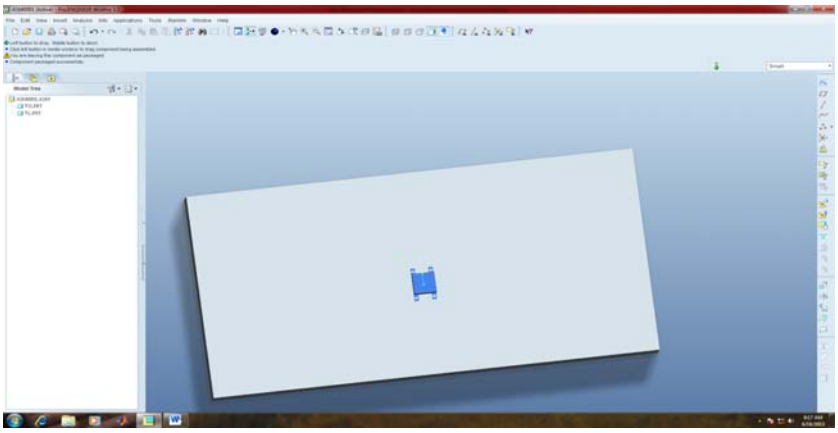

Figure 5-5: Center mounting location

5.3 Determination of Random Stresses by FE Analysis

The stress generated in the component is calculated using the ANSYS Transient Structural module. A CAD model of the mounted component is generated as shown in Fig 5-6.

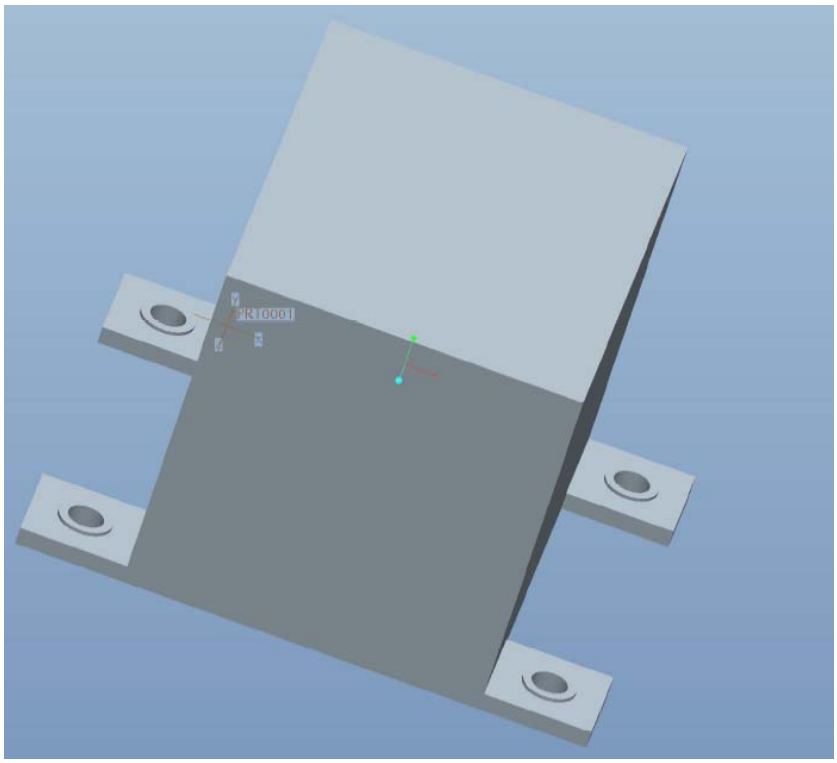

Figure 5-6: CAD model of vehicle mounted component

The component geometrical parameters are shown in Fig 5-7 and Fig 5-8.

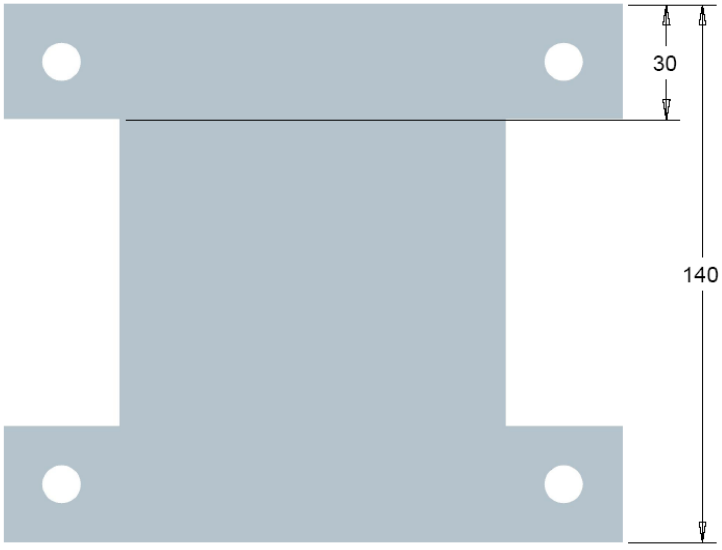

Figure 5-7: Bottom view of mounted component

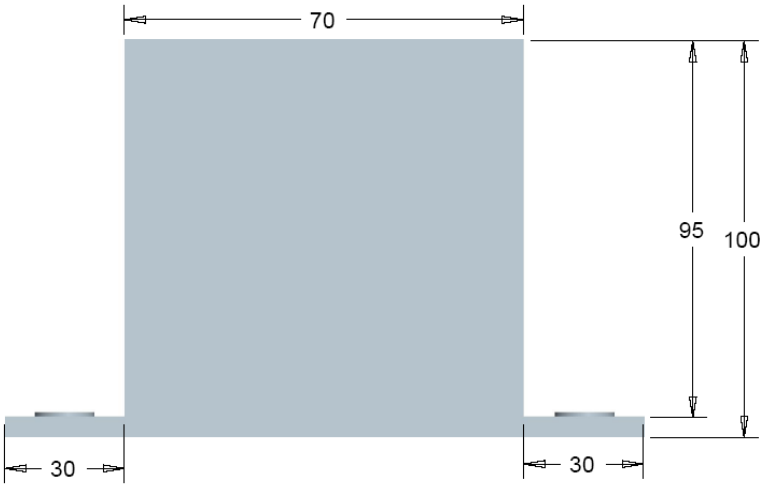

Figure 5-8: Front view of mounted component

5.3.5 Existing Methodologies of Fatigue Life Calculation of Vehicle Mounted Component

In the start, it was stated that the existing methodologies deal with the fatigue life calculation of vehicle mounted components. These are either experimental approaches or CAD based approaches, the difference between the two is only that in later technique the physical system is replaced by it's CAD model. Before embarking on the estimation of fatigue life of the component it becomes essential to have a brief overview of the existing methodologies. Broadly speaking, the fatigue life determination of vehicle mounted components fall into two main categories: time based approach and frequency based approach.

Time based approach makes use of the time signal of the load value acting at the component mounting point. This time varying load signal is then used to perform FE analysis of the CAD model of mounted component to the dynamic stress values in the component. These dynamic stress values are then used to calculate the fatigue life of mounted component. The work of is based on this approach. In this work fatigue life of the weldment of suspension support is performed. A CAD model of vehicle is excited by actual road profile in ADAMS software to know the dynamic load values, which are then used to perform the FE analysis of the part in ANSYS, which gives the stresses generated in the part. The stress profile in the part is shown in Fig 5-9.

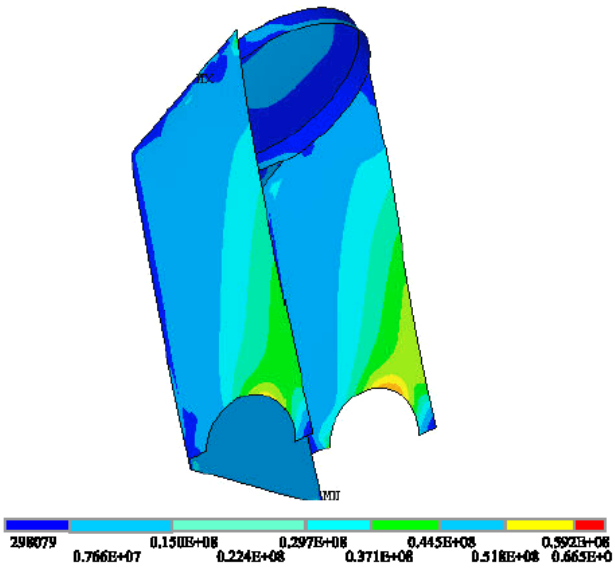

Figure 5-9: Stress profile in suspension support (reference [9])

The calculation of fatigue life follows the approach used to calculate fatigue life due to random stresses. First Rainflow counting algorithm is used to extract stress cycles of various magnitudes in the stress spectrum, and then Palmgren-Miner's rule is applied to know the fatigue life of part. Detail of this method will come later.

In the frequency based approach, the time signal of load is converted to it's PSD or power spectral density. The finite element analysis of the part is then carried out by applying the PSD of load to the part. The resulting stresses are also in the form of PSD.Basically, three kinds of stresses are obtained: 1-σ stress which acts for about 67% of time, 2-σ stress which acts for about 23% of time and 3-σ stress which acts for about 4% of time. Each of these stresses must be below the endurance limit of the material for the material to be safe. The work of is based on this approach. In this work the fatigue life of an auxiliary heater bracket is carried out. The stress profile generated in the material is shown in Fig 5-10.

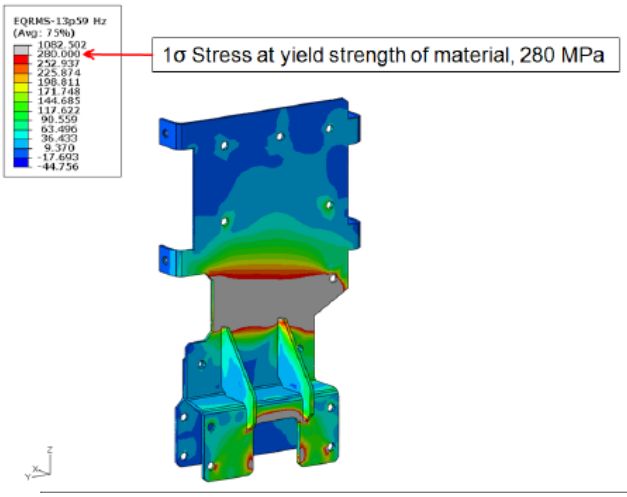

Figure 5-10: Stress profile in auxiliary heater bracket of truck (reference[6])

For the frequency domain analysis of fatigue, built in modules are available in finite element packages, such as Random Vibration module in ANSYS Workbench. By providing the input PSD to the part, the output results become available in the form of 1-σ, 2- σ and 3- σ stress distribution in the part. The time to failure in case any one of these stresses is below the material endurance limit is calculated by using the formula:

$$1\text{time} = \text{Number of cycles} / 105\ \text{Hz} / 68.3\%$$
$$2\text{time} = \text{Number of cycles} / 105\ \text{Hz} / 27.1\%$$
$$3\text{time} = \text{Number of cycles} / 105\ \text{Hz} / 4.33 \quad (5.1)$$

It was explained in chapter 1 that fatigue life calculation by this method is usually done for parts for which a recommended loading pattern is available. Such a loading pattern is for a few seconds of time and is usually standardized by the manufacturer of vehicle on which part has to be mounted. One such loading curve is given in reference[7].This loading curve with standard name of MIL-STD-810-F specifies the PSD of acceleration which the electric motor assembly of motor boat experiences.

For parts with no specified loading curve, the frequency domain method becomes slightly different and lengthy. The method used by Kagnici[15] is used. Here from the time signal of random load data input PSD of load signal is generated and is applied as input to the part. The statistical distribution of stresses in the form of PSD is obtained. Stress cycles of various magnitudes are calculated and finally fatigue life is calculated using Palmgren-Miner's rule of cumulative fatigue damage.Kagnici has used the approach to calculate fatigue life of vehicle body panels.

5.3.6 Limitations of Existing Methodologies with Reference to Present Study

It was stated in chapter 1 that detailed fatigue life evaluation is not the requirement of the present study. A rough estimation of fatigue life has to be made at various mounting locations of vehicle body for which a few seconds of stress data is required. This is obtained by carrying out the FE analysis of the component using the loads acting at component attachment points obtained by simulation of bond graph model generated in chapter 3 by the road profile generated in chapter 4.The component under consideration, unlike the component shown in Fig 5-9 is not constrained. So when the FE analysis is performed by applying 12 non uniform dynamic loads (3 at each mounting point), there is no constrained side to constraint the motion of component. Although, the motion of component remains constrained due to forces for a few time, however when the inertia effects become dominant the motion of component does not remains constrained due to forces. In ANSYS Transient Structural module, when this kind of situation is encountered, the solution stops. However, sufficient stress data becomes available which can be used to calculate an estimated fatigue life.

The purpose of the present study is not to calculate fatigue life accurately; rather variation of fatigue life or variation in the magnitude of dynamic stresses is to be studied so that we may come up with a suitable mounting location of the component. From the stress spectrum obtained from FE analysis a rough estimation of fatigue lives can be obtained for various mounting

locations and the variation of fatigue life with the change of mounting location will become known. By studying such a variation we can identify the zone on vehicle body where the component's fatigue life would be close to maximum. Determination of actual fatigue life value at such location can then be carried out using experimental means.

5.3.7 Load Values Acting at Component Mounting Points

The Bond Graph model generated in chapter is simulated by the road profile generated in chapter. In the present study road profile is assumed to be ergodig.This means that the left and the right wheels see same input. For a vehicle travelling on a highway, this type of road input is satisfactory, although for cases like vehicle travelling in off road conditions, a 2D road profile which models the road profile in x directions has to be used. The forces generated at the component mounting points for CG mounting locations are shown in Fig 5-11.

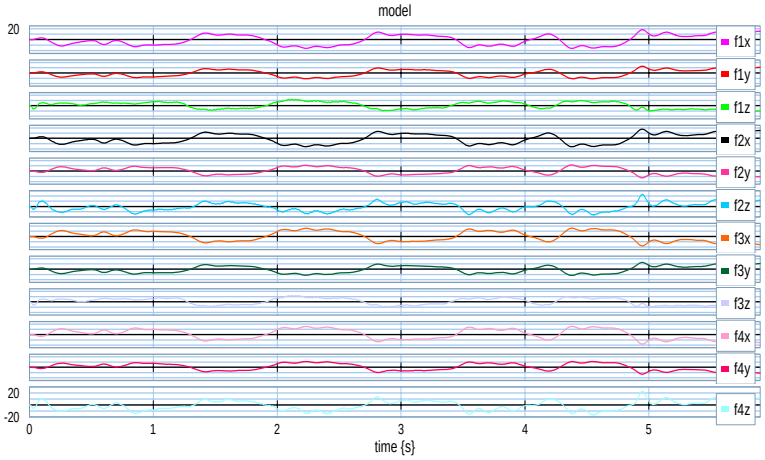

Figure 5-11: Load values at component mounting points

5.3.8 Preprocessing and Meshing Details

The material used is AISI-1040 and the values of mechanical and fatigue properties of the material are given in table 5. These values along with the random stress data are given as input to the fatigue calculation software StoFlo, and the fatigue results are thus obtained. The load values as obtained by 20Sim are transferred to ANSYS Transient Structural module. The forces are applied to the CAD model of the component in the transient structural module. As the association of a particular force with a particular corner of component is known, hence forces must be applied at proper locations on the component. Also the sign convention must not be

violated, or else incorrect results would be obtained. The CAD model of the component with forces applied is shown in Fig 5-12.As component is bolted to the vehicle body through anti vibration mounts, the forces acting on component are distributed on a circular area equal to area under bolt head. Thus force vector at each corner acts on a finite area as shown in Fig 5-8.The diameter of the bolt head in the present case is 1.5cm.The nominal diameter of the bolts used to connect the component to the anti vibration mounts is 1cm.

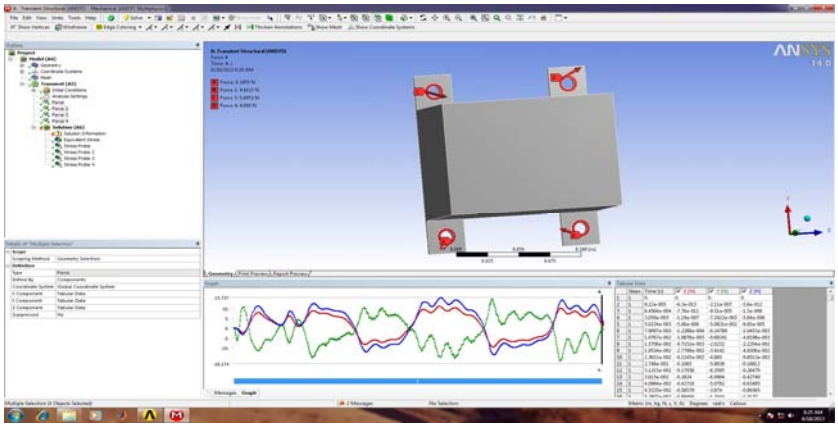

Figure 5-12: CAD model of component in ANSYS transient structural with forces applied

The fatigue constants of the material are shown in the table 5-1.These constants are used in the stress life formulas used in the calculation of fatigue life.

Table 5-1: Fatigue constants of component material

S_u	931MPa
B	-0.07
E	200000Mpa
K`	1434Mpa
n`	0.14
c	-0.69
K_f`	1
σ_f	1330
ε_f`	0.66
σ_f`	1240Mpa

The dynamic stresses generated in the component due to the load values acting at the attachment points, are calculated by dynamic simulation of a CAD model of the mounted component in ANSYS.

The stress profile generated in the component is shown in Fig 5-15, along with the mesh used to discretize the component. The meshed has been fined at edges up to extent where the results converge. The number of elements now increases to 20419 from the previous number of 1965.The difference between the stresses calculated for coarse and fine mesh is shown in Fig 5-13 for one of the stress probe locations. In Fig 5-14, the stresses calculated when mesh is further refined (depth level 3) are compared with the stresses values obtained for depth level 2.It is seen that there is no difference between the values of stresses for the two mesh sizes. Hence mesh size with depth level 2 can be used for the fatigue life calculations. The mesh refinement is made using ANSYS workbench mesh refinement tool.

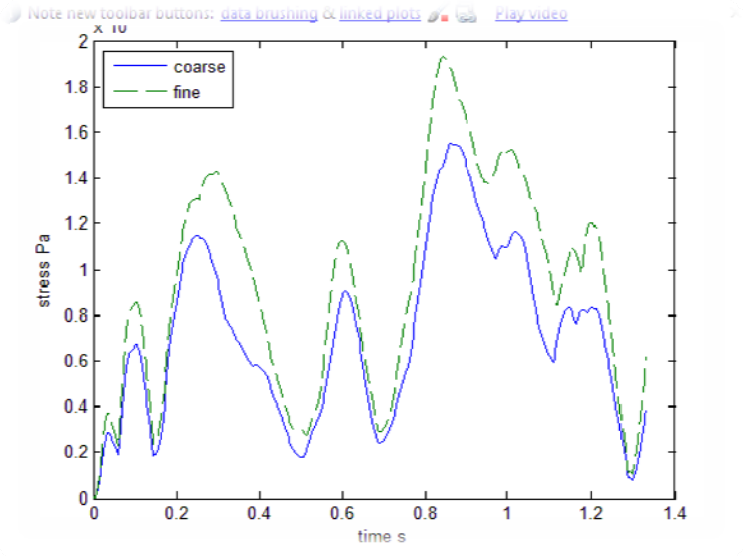

Figure 5-13: Difference between stresses calculated for coarse and fine(level 2) meshes

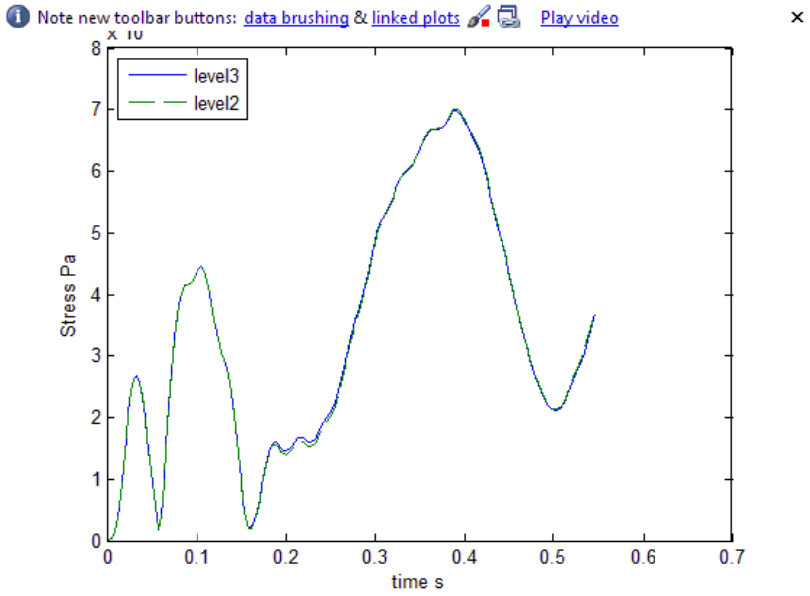

Figure 5-14: Difference between stresses for stress level 2 and 3

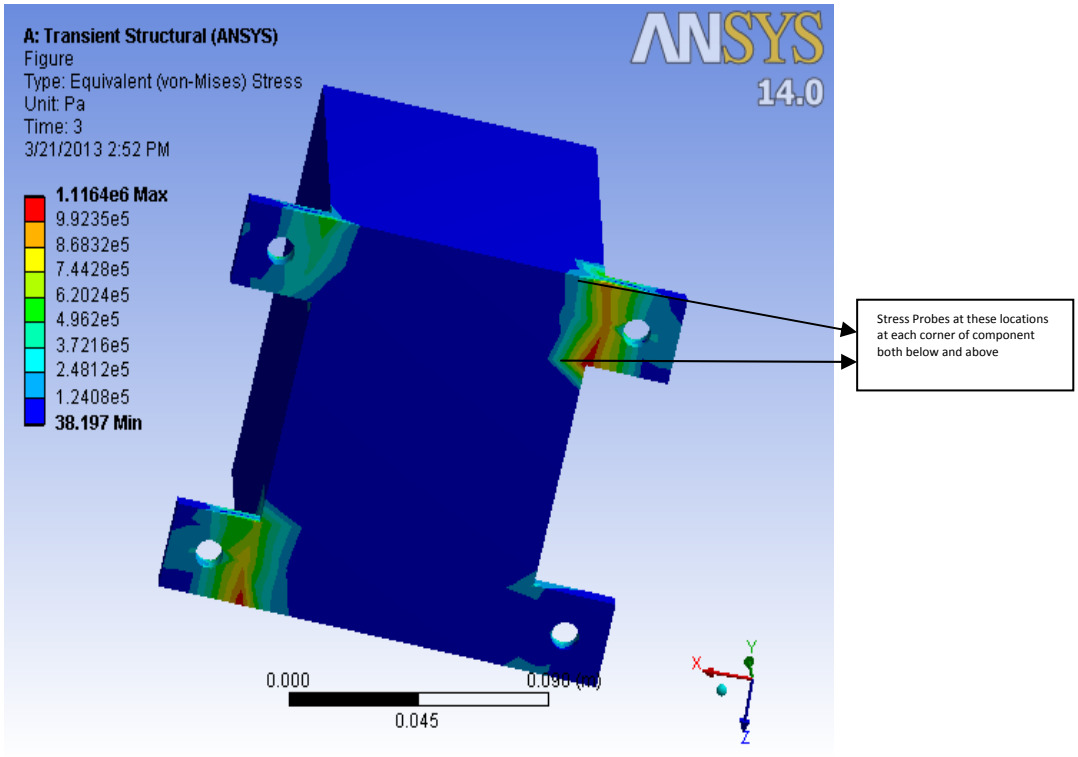

Figure 5-15: Stress profile in attached part

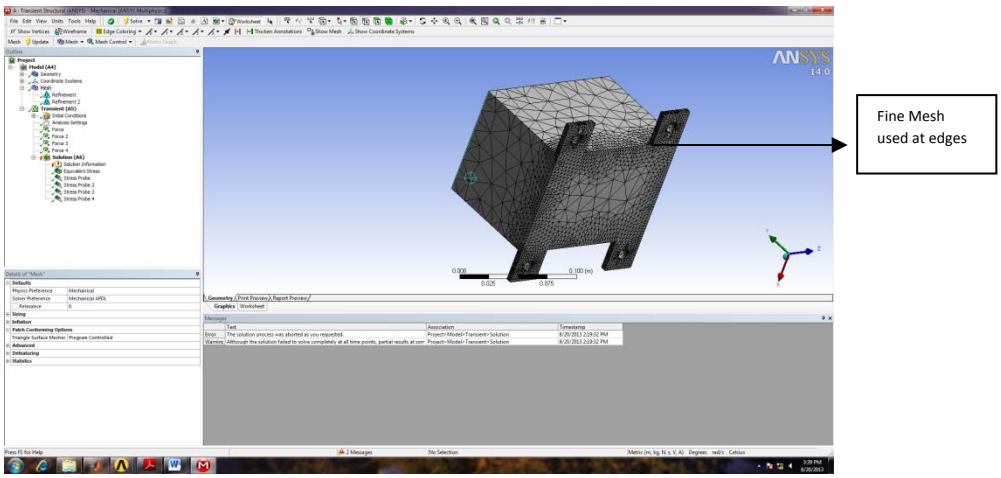

Figure 5-16: Screenshot from ANSYS showing mesh fined at edges

5.3.9 Stress Results

The stresses generated in the component are shown in Fig 5-17-Fig 5-19.The measurement of stresses is made at the edges at 16 locations by using stress probes (4 at each corner).The stresses are measured at these locations as maximum stresses appear at these points. The fatigue life is measured for all these stress values and the minimum of these is then selected for the results.

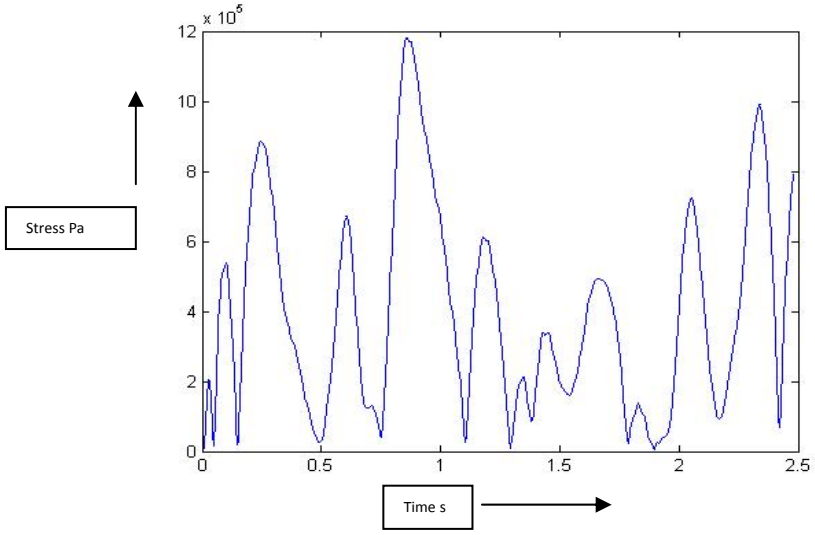

Figure 5-17: Stress profile for CG mounting location

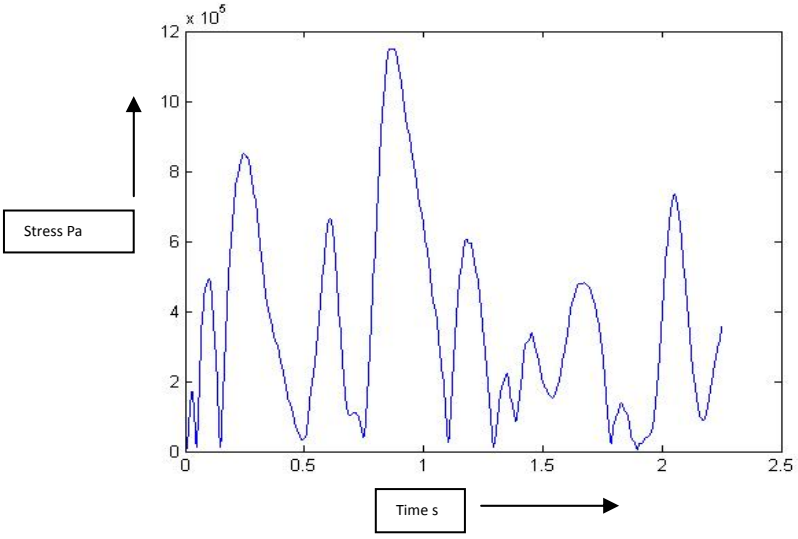

Figure 5-18: Stress profile for center mounting location

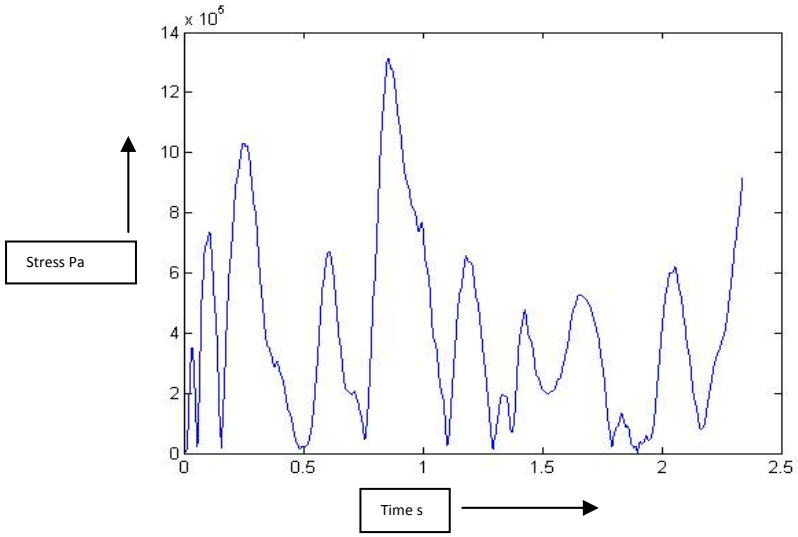

Figure 5-19: Stress profile for front mounting location

It must be emphasized at this point that force values used are those in the inertial coordinate system.

5.4 Fatigue Life Estimation of Component

The dynamic stress values generated at the mounts are a basis of the fatigue life assessment. These stresses, although cyclic, are non uniform and thus the fatigue life cannot be assessed by merely looking at the S-N curve of the material. At this stage Rain flow counting algorithm[18] is applied to this stress data so that the number of stress cycles of various amplitudes become known. Once this is done Palmgren-Miner's rule of cumulative stress damage is used to estimate the fatigue life of the component. The complete process of stress cycles calculation and fatigue life estimation is done automatically by Stoflo_10.08, an excel application. Once provided with the stress data from the ANSYS simulation, the component fatigue life, in terms of the number of repetitions of the input excitation signal, is calculated.

The Palmgren-Miner's rule of cumulative fatigue damage is expressed as:

$$\frac{n1}{N_{r1}} + \frac{n2}{N_{r2}} + \cdots + \frac{nn}{N_{rn}} = \sum \frac{ni}{N_{ri}} = C \qquad (5.2)$$

Here ni is the number of cycles of the applied stressσi, N_{ri} is the number of the cycles of stress stateσi which will cause failure of the component due to fatigue. C is usually taken as one. The applied stress cycles can be determined by using the Rainflow counting algorithm. An Excel

module Stoflo^{TM} [13] is used for the purpose. When provided with the stress data, it uses Rainflow counting algorithm and gives values of σi the results obtained are shown in Table 6.After Rainflow counting algorithm is applied, the software calculates the component fatigue life using Palmgren-Miner's Rule of cumulative fatigue damage. All we have to do is to input the material coefficients and the random stress data.

$$B_f \sum \frac{ni}{N_{ri}} = 1 \tag{5.3}$$

Here B_f is the number of repetitions of applied alternative loads.

The allowable stress cycles N_{ri} depend on the fatigue life equation we use. In the present analysis we use stress life equation to determine the allowable cycles

$$S_{Nf}=A(N_f)^B \tag{5.4}$$

S_{Nf} is determined using the modified Goodman Equation:

$$\frac{S_a}{S_{NF}} + \frac{S_m}{S_u} = 1 \tag{5.5}$$

S_a is the average stress in a cycle. S_u is the ultimate tensile strength of material, S_m is the mean stress. Stress life approach is used when the generated stresses are well below the elastic limit of material and the cycles to failure are large[8].The curves of stress versus cycles to fatigue failure are called S-N curves or Wohler curves[23].

Finally using the Palmgren Miner's rule, the fatigue life is determined.

$$B_f \sum \frac{ni}{N_{ri}} = 1 \tag{5.6}$$

The fatigue life of the component is determined in terms of the value of the termB_f.Since crack initiation time is being used as the fatigue life of the component, value of B_f must be indicative of the fatigue life as crack initiation time. The results of component fatigue life at four mounting locations of vehicle are as follows:

Table 5-2: Estimated fatigue life results for various mounting locations

Fatigue Life in Numbers of Hours	Mounting Location
3.5561e+21	Corner
6.7513e+21	Front
6.8503e+021	CG
8.3125e+021	Center

It is seen that the fatigue life is maximum at the center mounting location of the component. We shall now investigate the cause of fatigue life variation at various mounting locations on vehicle body with the help of modal analysis.

5.5 Determination of Feasible Mounting Location Using Modal Analysis

The modal analysis of the full car model is carried out to know the dominant modes. There are three dominant modes. The eigenvalues which are greater than 5 times the first eigen value are assumed to play no part in the overall response[24]. Thus there are three modes which are dominant. Modes are calculated by using the MATLAB command eig(A), where A is the characteristic matrix in the state space formulation. The output consists of a eigenvalue matrix and a eigenvector matrix. Mode shape can be found by using the eigenvector corresponding to a eigenvalue.The eigenvector consists of values of states. To excite any particular mode, the eigenvector values are used as initial values. Also the eigenvectors always exist in complex conjugate pairs. Now, how these complex conjugate modes combine to give real motions has to be understood.

For nth mode, the motion in that mode is defined as the sum of motions due to two conjugate eigenvalues/eigenvectors. Now we write mathematically[22]:

$$\boldsymbol{x}(t) = e^{\lambda_{n1}t}\boldsymbol{x}_{n1} + e^{\lambda_{n2}t}\boldsymbol{x}_{n2}$$

$$= e^{\lambda_{n1}t}\boldsymbol{x}_{n1} + e^{\lambda_{n1}{}^{*}}x_{n1}{}^{*}$$

$$= e^{(\sigma_{n1}+j\omega_{n1})t}\boldsymbol{x}_{n1} + e^{(\sigma_{n1}-j\omega_{n1})t}x_{n1}{}^{*}$$

$$=2e^{\sigma_{n1}t}Re(\boldsymbol{x}_{n1}) \quad (5.7)$$

Thus the imaginary components of eigenvectors cancel each other as they rotate counterclockwise, while the real components add. In this way we have real motion from complex eigenvectors.In the equation 5.7, λ denotes the eigen value.

1. *Mode Shape at Eigen Value -3.0337+ - 6.9873i:* This is the most significant mode. This is a pure rolling mode. The roll motion is such that the front left and rear left corners of vehicle body move in the negative z direction by amount 0.00045029, while the front right and rear right move in the positive z direction by the same amount. The mode shape is shown pictorially in Fig 5-20.

2. *Mode Shape at Eigen Value -4.6844 +- 9.3574i:* This is the second significant mode. At this mode the motion is combination of bounce and pitch motions. The CG moves in the negative z direction by amount 0.0335. The front side moves in the negative z direction by amount 0.0571 and the rear side moves in the positive z direction by 0.0004877.The mode shape is shown pictorially in Fig 5-21.

3. *Mode Shape at Eigen Value -6.1241 +- 7.4338i:* This is the third significant mode and also the motion is combination of bounce and pitch. The pitch is now opposite to the pitch motion of mode2.The CG moves in the negative z direction by 0.0474, and the front side moves in the negative z direction by-0.0004923, while the rear side moves in negative z direction by 0.1147. The mode shape is shown pictorially in Fig 5-22.

Table 5-3: Significant mode values for three significant eigenvalues

Modes at Eigen Value	Front Left Corner Displacement	Displacement of CG
-3.0337+-6.9873i	-0.0004509	0
-4.6844+-9.3574i	-0.0571	-0.0335
-6.1241+-7.4338i	-0.0004923	-0.0474

The input road profile is composed of frequencies, such that the PSD of frequencies decrease from the lowest frequency to the highest frequency. This means that the most dominant

mode will be excited most as it also receives the frequency with highest PSD. In this case the pure rolling mode will be excited the most, followed by the mode 2 and mode 3.The combined effect of these three modes is that the front left corner has the greatest displacement, while displacements decrease as we move from the front left corner to the front side and from the front side to the CG and the geometric center of the vehicle. The modes are pictorially represented below:

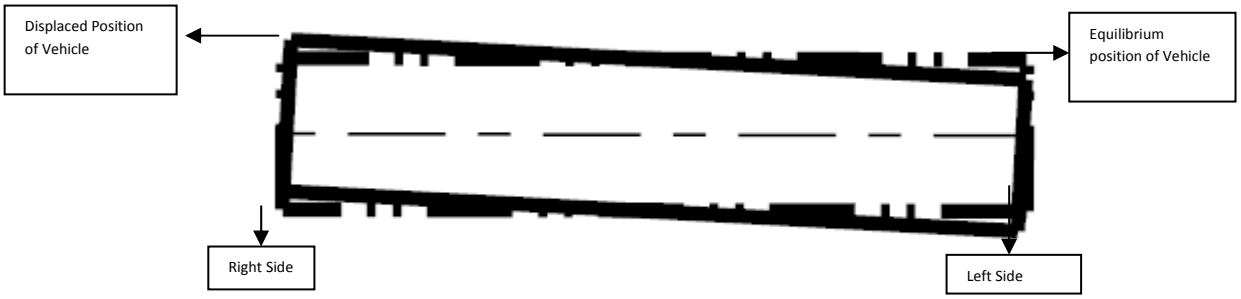

Figure 5-20: First significant mode, vehicle viewed from front

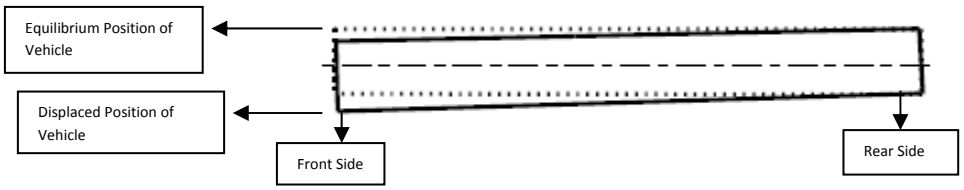

Figure 5-21: Second significant mode vehicle viewed from left

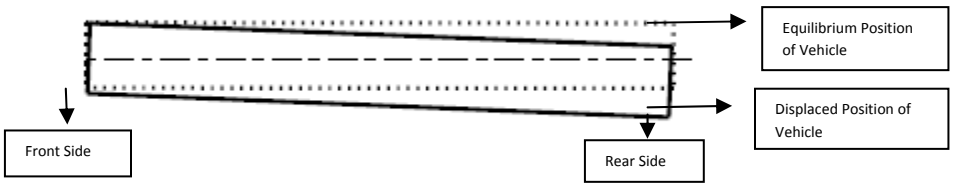

Figure 5-22: Third significant mode vehicle viewed from left

Now in vibration systems, greater displacement means greater energy level associated with the point undergoing displacement, so we deduce that in our case, when the component is attached at front left corner it receives the greatest energy and when the component is attached at the geometric center of vehicle body, it receives the lowest energy. Thus greater the energy received, greater the generated stresses and vice versa. In this way by carrying out modal analysis we can determine the most feasible mounting location by knowing which point on vehicle body undergoes minimum displacement.

This point can be proved by checking the power level associated with a particular point on vehicle body. Two points, one at the front left corner and one at the CG are selected and power signal is found at the these two points. The Fig 5-23 show the PSD of power signal at the front left corner and the Fig 5-24 shows the power signal PSD at the CG of vehicle body. It is seen that the PSD of power signal associated with the front left corner is greater as compared to that of the geometric center.

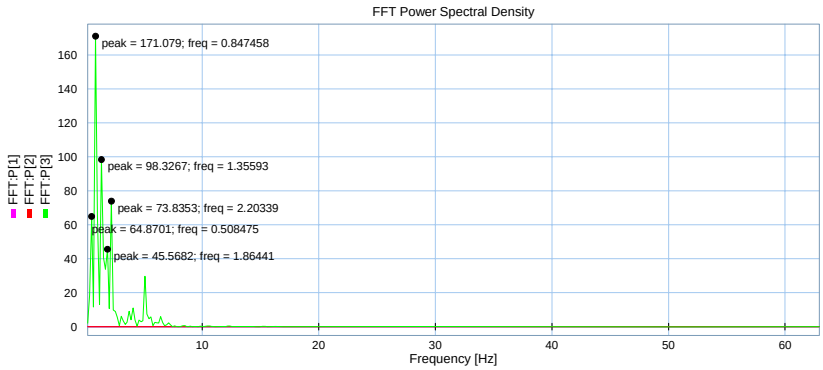

Figure 5-23: PSD of power signal at corner

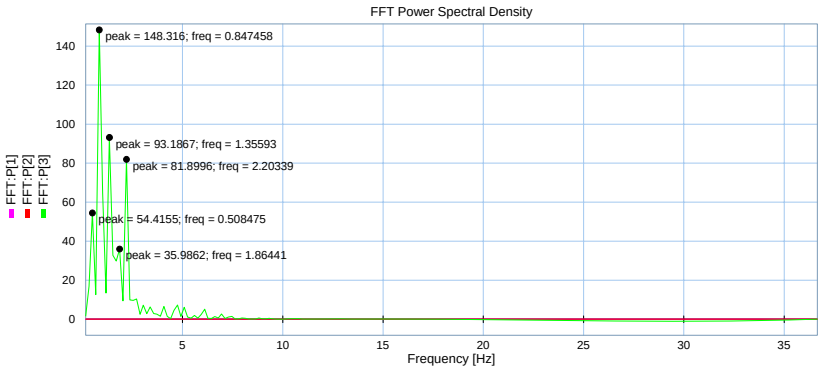

Figure 5-24: PSD of power signal at CG

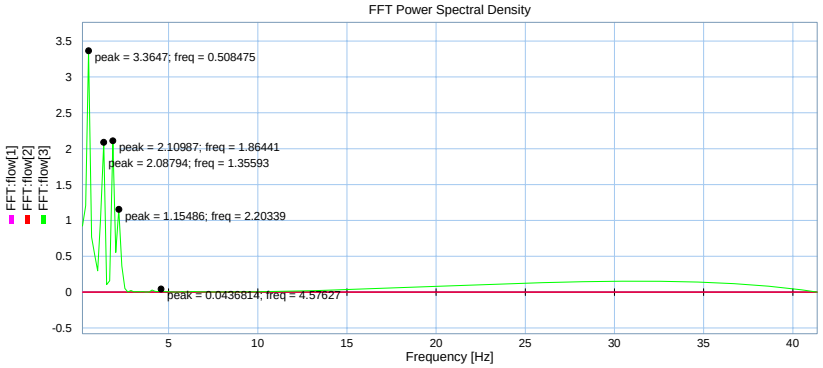

Figure 5-25: PSD of velocity signal at CG

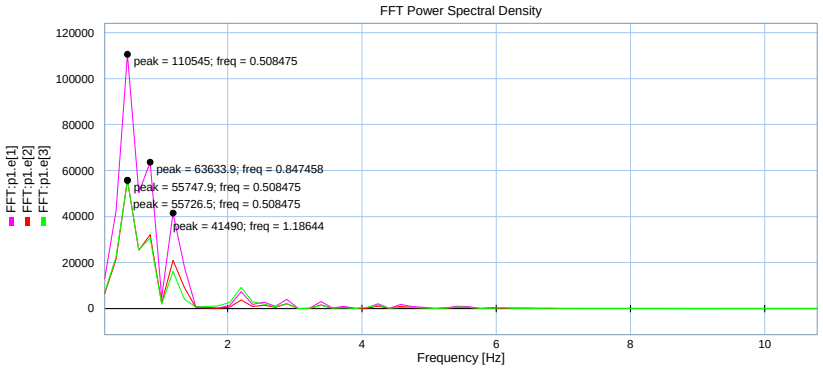

Figure 5-26:PSD of effort signal at CG

It is seen from the above figures that for both the force and velocity at the point under consideration on vehicle body the maximum value of PSD occurs at the frequency value of 0.508475, while for power signal it occurs at the frequency value of 0.847458.The reason for this

is that since power is the product of force and velocity signal hence the product produces maximum value of PSD at frequency value of 0.847458.

5.6 Conclusion

The objective of this work is to study the variation occurring in fatigue life of vehicle mounted components by changing component mounting location. It is seen that the fatigue characteristics can be studied for various mounting locations and suspension parameter values. Same study carried out using experimental or CAD means would have taken a lot of time. Thus for preliminary design estimation the developed framework can be used in place of experimental or CAD means, and once suitable location on vehicle body has been identified, the detailed fatigue life of component can be determined using existing methodologies. Moreover, a study of significant modes of vehicle helps to identify the area of vehicle body where attached component will be safe. This saves the time by limiting the number of locations where the fatigue life estimation of the component is to be performed. Thus it can be said that the developed framework has increased the usefulness of the current methodologies of fatigue life evaluation of vehicle mounted components in that the detailed fatigue life evaluation of vehicle mounted components can now be carried out at locations where the component placement will result in maximum fatigue life of the component.

CHAPTER 6: Summary and Suggestions for Future Work

In this study, fatigue life characteristics of a component mounted on a vehicle body have been studied. For this purpose model of a full car suspension, which includes vehicle suspension system along with a part attached to vehicle body, has been generated using bond graph method. The model allows the determination of forces available at the mounting points of attached part, as vehicle travels on road. These force values are then used for fatigue analysis of attached part. The stresses generated in the part are determined by performing finite element analysis of part using known force values in ANSYS.Rainflow counting algorithm is then used to extract stress cycles of various magnitudes from non-uniform stress data, and finally application of Palmgren Miner's rule gives the part fatigue life**.** The process is repeated by changing mounting locations of part on vehicle body and the optimum mounting location; where the part experiences maximum fatigue life, is determined.

It is seen that use of bond graph method greatly simplifies model generation and model modification. The graphical nature of bond graph method makes it easy to understand working of a bond graph model. Any kind of modification occurring in the physical model like change of component mounting location, change of suspension parameters of vehicle, change of anti-vibration mount properties are incorporated in the bond graph model merely by changing parameter values. Similarly, if any kind of modification/augmentation occurs in the physical model, like change of number of attachment points, attachment of more than one component on vehicle etc, the bond graph model can be accordingly modified. Like state space model constructed from the governing differential equations, there is no need to generate a new model.

There is a great deal of scope regarding future work. For greater fatigue life improvement, the model can be modified to active and semi active suspensions. By incorporation of controller in the suspension, the dangerous modes can be eliminated from the dynamics of the vehicle. Semi active suspension in the form of skyhook controller is well researched and developed for passenger vehicles. It's use for the purpose of fatigue life improvement can be explored.

The present work is limited to studying the fatigue life variation of the component by varying component mounting location. However, since fatigue life is also dependent on other parameters like anti-vibration mount properties, and suspension parameters; effect of these parameters on component fatigue life can be studied as part of future work.Infact, selection of optimum anti vibration mounts which effectively isolate the dangerous modes is a promising area in which work can be done.

In the present study ergodic road profile has been used. Thus left and right wheels of the vehicle receive the same input. Further improvement in the results can be obtained if we use a 2D road profile as described in the work of[21]. This kind of road profile varies in the x and y direction. Application of such a road profile as input to the vehicle simulates a more realistic scenario.

Appendix

Appendix-A

A state space model of full car suspension in MATLAB

```
kt=200000;  %Stiffness of Wheels
mp=100;      %Mass of Passenger Seat
m=1100;      %Vehicle Mass
m1=85;       %Front Tire Mass
m3=m1;
m2=60;       %Rear Tire Mass
m4=m2;
ix=400;      %Moment of Inertia for Roll
iy=2400;     %Moment of Inertia for Pitch
w1=1;        %Distance of CG from Left Side
w2=0.5;      %Distance of CG from Right Side
a=1.4;       %Distance of CG from Rear Side
b=1.2;       %Distance of CG from Front Side
xp=0.25;     %x Distace of Passenger Seat from CG
yp=0.375;    %y Distace of Passenger Seat from CG
kp=90000;    %Passenger Seat Stiffness
cp=2500;     %Passenger Seat Damping
k1=40000;    %Front Suspension Stiffness
k3=k1;
k2=32000;    %Front Suspension Stiffness
k4=k2;
c4=2500;     %Rear Suspension Damping
c2=c4;
c1=2500;     %Front Suspension Damping
c3=c1;
```

```
A = [ 0 1 0 0 0 0 0 0 0 0 0 0 0 0 0 0;
    -kp/mp  -cp/mp  kp/mp  cp/mp  0 0 0 0 0 0 0 0 (kp*xp)/mp   (cp*xp)/mp  (-
yp*kp)/mp  (-cp*yp)/mp;
   0 0 0 1 0 0 0 0 0 0 0 0 0 0 0  0;
   kp/m  cp/m   (-k1-k2-k3-k4-kp)/m  (-c1-c2-c3-c4-cp)/m  k1/m  c1/m  k2/m
c2/m  k3/m c3/m  k4/m  c4/m ((k1*a)-(k2*b)+(k3*a)-(k4*b)-(kp*xp))/m  ((c1*a)-
(c2*b)+(c3*a)-(c4*b)-(cp*xp))/m      ((-k1*w1)-
(k2*w2)+(k3*w1)+(k4*w2)+(kp*yp))/m     ((-c1*w1)-
(c2*w2)+(c3*w1)+(c4*w2)+(cp*yp))/m;
   0 0 0 0 0 1 0 0 0 0 0 0 0 0 0 0;
   0  0 k1/m1  c1/m1  (-k1-kt)/m1  -c1/m1 0 0 0 0 0 0  -(k1*a)/m1  -(c1*a)/m1
(k1*w1)/m1  (c1*w1)/m1;
   0  0 0 0 0 0 0 1 0 0 0 0 0 0 0 0;
   0  0 k2/m2  c2/m2  0 0 (-k2-kt)/m2  -c2/m2  0 0 0 0 (k2*b)/m2  (c2*b)/m2
(k2*w2)/m2  (c2*w2)/m2;
   0 0 0 0 0 0 0 0 0 1 0 0 0 0 0 0;
   0  0 k3/m3  c3/m3 0 0 0 0 (-k3-kt)/m3  -c3/m3 0  0  -(k3*a)/m3  -(c3*a)/m3
-(k3*w1)/m3  -(c3*w1)/m3;
   0  0 0 0 0 0 0 0 0 0 0 1 0 0 0 0;
   0  0 k4/m4  c4/m4 0 0 0 0 0 0 (-k4-kt)/m4  -c4/m4  (k4*b)/m4  (c4*b)/m4  -
(k4*w2)/m4  -(c4*w2)/m4;
   0  0  0 0 0 0 0 0 0 0 0 0 0 1 0 0;
   -(xp*kp)/iy  -(xp*cp)/iy    ((a*k1)-(b*k2)+(a*k3)-(b*k4)+(xp*kp))/iy
((a*c1)-(b*c2)+(a*c3)-(b*c4)+(xp*cp))/iy   -(a*k1)/iy  -(a*c1)/iy  (b*k2)/iy
(b*c2)/iy  -(a*k3)/iy  -(a*c3)/iy  (b*k4)/iy  (b*c4)/iy  ((-a*a*k1)-(b*b*k2)-
(a*a*k3)-(b*b*k4)+(xp*xp*kp))/iy     ((-a*a*c1)-(b*b*c2)-(a*a*c3)-
(b*b*c4)+(xp*xp*cp))/iy   ((a*w1*k1)-(b*w2*k2)-(a*k3*w1)+(b*k4*w2)-
(xp*yp*kp))/iy    ((a*w1*c1)-(b*w2*c2)-(a*c3*w1)+(b*c4*w2)-(xp*yp*cp))/iy;
   0 0 0 0 0 0 0 0 0 0 0 0 0 0 0 1;
   -(yp*kp)/ix  -(yp*cp)/ix  ((-w1*k1)-(w2*k2)+(w1*k3)+(w2*k4)+(yp*kp))/ix
((-w1*c1)-(w2*c2)+(w1*c3)+(w2*c4)+(yp*cp))/ix  (w1*k1)/ix   (w1*c1)/ix
(w2*k2)/ix (w2*c2)/ix  (-w1*k3)/ix  (-w1*c3)/ix  (-w2*k4)/ix  (-w2*c4)/ix
((w1*k1*a)-(w2*k2*b)-(w1*k3*a)+(w2*k4*b)+(yp*kp*xp))/ix      ((w1*c1*a)-
(w2*c2*b)-(w1*c3*a)+(w2*c4*b)+(yp*cp*xp))/ix   ((-w1*w1*k1)-(w2*w2*k2)-
(w1*w1*k3)-(w2*w2*k4)-(yp*yp*kp))/ix    ((-w1*w1*c1)-(w2*w2*c2)-(w1*w1*c3)-
(w2*w2*c4)-(yp*yp*cp))/ix;];
```

```
B=[ 0 0 0 0;
    0 0 0 0;
    0 0 0 0;
    0 0 0 0;
    0 0 0 0;
    kt/m1 0 0 0;
    0 0 0 0;
    0 kt/m2 0 0;
    0 0 0 0;
    0 0 kt/m3 0;
    0 0 0 0;
    0 0 0 kt/m4;
    0 0 0 0;
    0 0 0 0;
    0 0 0 0;
    0 0 0 0;]

C=[0 0 1 0 0 0 0 0 0 0 0 0 0 0 0 0;]

D=[0]

%state space model

sys=ss(A,B,C,D)

t=0:0.01:10

%input applied at the front wheels

u2=-0.15*(t>=1&t<=3)

u4=u2;

%input applied at the front wheels

u3=-0.15.*(t>=7&t<=9)
```

```
u1=u3;

u=[u1' u2' u3' u4']

plot(t,u)

lsim(sys,u,t)
```

Appendix-B

State space model of the full car suspension (chapter).The model is similar to that of appendix-a with the difference that the passenger seat mass is taken as zero; so that a model of full car suspension without passenger seat is generated. The outputs of the bond graph model of full car suspension (page 36) is compared with the output of this model.

```
kt=200000;  %Stiffness of Wheels
mp=0;      %Mass of Passenger Seat
m=1100;      %Vehicle Mass
m1=85;       %Front Tire Mass
m3=m1;
m2=60;       %Rear Tire Mass
m4=m2;
ix=400;      %Moment of Inertia for Roll
iy=2400;     %Moment of Inertia for Pitch
w1=1;        %Distance of CG from Left Side
w2=0.5;      %Distance of CG from Right Side
a=1.4;       %Distance of CG from Rear Side
b=1.2;       %Distance of CG from Front Side
xp=0;     %x Distace of Passenger Seat from CG
yp=0;    %y Distace of Passenger Seat from CG
kp=90000;    %Passenger Seat Stiffness
cp=2500;     %Passenger Seat Damping
k1=40000;    %Front Suspension Stiffness
k3=k1;
k2=32000;    %Front Suspension Stiffness
k4=k2;
c4=2500;     %Rear Suspension Damping
c2=c4;
c1=2500;     %Front Suspension Damping
c3=c1;
```

```
A = [

    0 1 0 0 0 0 0 0 0 0 0 0  0;
      (-k1-k2-k3-k4-kp)/m  (-c1-c2-c3-c4-cp)/m  k1/m  c1/m  k2/m  c2/m  k3/m
c3/m  k4/m  c4/m ((k1*a)-(k2*b)+(k3*a)-(k4*b)-(kp*xp))/m  ((c1*a)-
(c2*b)+(c3*a)-(c4*b)-(cp*xp))/m      ((-k1*w1)-
(k2*w2)+(k3*w1)+(k4*w2)+(kp*yp))/m     ((-c1*w1)-
(c2*w2)+(c3*w1)+(c4*w2)+(cp*yp))/m;
    0 0 0 1 0 0 0 0 0 0 0 0 0 0;
    k1/m1  c1/m1  (-k1-kt)/m1  -c1/m1 0 0 0 0 0 0  -(k1*a)/m1  -(c1*a)/m1
(k1*w1)/m1  (c1*w1)/m1;
    0 0 0 0 0 1 0 0 0 0 0 0 0 0;
    k2/m2  c2/m2  0 0 (-k2-kt)/m2  -c2/m2  0 0 0 0 (k2*b)/m2  (c2*b)/m2
(k2*w2)/m2  (c2*w2)/m2;
    0 0 0 0 0 0 0 1 0 0 0 0 0 0;
    k3/m3  c3/m3 0 0 0 0 (-k3-kt)/m3  -c3/m3 0  0  -(k3*a)/m3  -(c3*a)/m3  -
(k3*w1)/m3  -(c3*w1)/m3;
    0 0 0 0 0 0 0 0 0 1 0 0 0 0;
    k4/m4  c4/m4 0 0 0 0 0 0 (-k4-kt)/m4  -c4/m4  (k4*b)/m4  (c4*b)/m4  -
(k4*w2)/m4  -(c4*w2)/m4;
     0 0 0 0 0 0 0 0 0 0 0 1 0 0;
       ((a*k1)-(b*k2)+(a*k3)-(b*k4)+(xp*kp))/iy    ((a*c1)-(b*c2)+(a*c3)-
(b*c4)+(xp*cp))/iy   -(a*k1)/iy  -(a*c1)/iy  (b*k2)/iy  (b*c2)/iy  -(a*k3)/iy
-(a*c3)/iy  (b*k4)/iy  (b*c4)/iy  ((-a*a*k1)-(b*b*k2)-(a*a*k3)-
(b*b*k4)+(xp*xp*kp))/iy     ((-a*a*c1)-(b*b*c2)-(a*a*c3)-
(b*b*c4)+(xp*xp*cp))/iy   ((a*w1*k1)-(b*w2*k2)-(a*k3*w1)+(b*k4*w2)-
(xp*yp*kp))/iy    ((a*w1*c1)-(b*w2*c2)-(a*c3*w1)+(b*c4*w2)-(xp*yp*cp))/iy;
    0 0 0 0 0 0 0 0 0 0 0 0 0 1;
     ((-w1*k1)-(w2*k2)+(w1*k3)+(w2*k4)+(yp*kp))/ix   ((-w1*c1)-
(w2*c2)+(w1*c3)+(w2*c4)+(yp*cp))/ix  (w1*k1)/ix   (w1*c1)/ix  (w2*k2)/ix
(w2*c2)/ix  (-w1*k3)/ix  (-w1*c3)/ix  (-w2*k4)/ix  (-w2*c4)/ix  ((w1*k1*a)-
(w2*k2*b)-(w1*k3*a)+(w2*k4*b)+(yp*kp*xp))/ix      ((w1*c1*a)-(w2*c2*b)-
(w1*c3*a)+(w2*c4*b)+(yp*cp*xp))/ix   ((-w1*w1*k1)-(w2*w2*k2)-(w1*w1*k3)-
(w2*w2*k4)-(yp*yp*kp))/ix    ((-w1*w1*c1)-(w2*w2*c2)-(w1*w1*c3)-(w2*w2*c4)-
(yp*yp*cp))/ix;];
```

```
B=[
    0 0 0 0;
    0 0 0 0;
    0 0 0 0;
    kt/m1 0 0 0;
    0 0 0 0;
    0 kt/m2 0 0;
    0 0 0 0;
    0 0 kt/m3 0;
    0 0 0 0;
    0 0 0 kt/m4;
    0 0 0 0;
    0 0 0 0;
    0 0 0 0;
    0 0 0 0;]

C=[ 0 0 0 0 0 0 0 0 0 0 0 1 0 0;]

D=[0]

sys=ss(A,B,C,D)
t=0:0.01:10

h=1.*t.*(t>=0&t<1);

u1=1.*(t>=1&t<=10);

u1=u1+h;

u2=-0.*(t>=1&t<=3)

u4=u2;

u3=u1;

u=[u1' u2' u3' u4']
```

```
plot(t,u)

lsim(sys,u,t)
```

Appendix-C

Matlab Program to generate random road profile. This program is reproduced here exactly as it appears in the work of Kailas V.Inamdar[12].

```
% function[U,t]=rough_road_input(N,H)
% Generates N points in time U(t) at a time interval of H with zero
mean.
% N must be a power of 2! The N points will be generated
% so as to have a desired one-sided PSD defined in the function
% road_psd_smooth_highway(f). f is the frequency in Hertz. The
frequency resolution will be 1/NH. The smallest frequency will be 0
Hz and the largest frequency will be 1/2H Hz. Note, the frequency
1/2H is referred to as the folding frequency.

function[U,t]=rough_road_input(N,H)

no2=N/2;

% Step 1: Generate frequencies and PSD values at each frequency

f=0:1/(N*H):1/(2*H);

%Note, the first frequency is zero but we don't
%compute GY at f=0 to avoid potential computational problems. GY at
f=0
%should be zero for a zero mean process.
GU(1)=0;
% If the desired PSD is defined in road_psd_smooth_highway, then use
the next 3 lines.

for m1=2:no2+1
% USE NEXT LINE IF SIMULTAION IS FOR SMOOTH RUNWAY
%GU(m1)=road_psd_smooth_runway(f(m1));
% USE NEXT LINE IF SIMULTAION IS FOR ROUGH RUNWAY
%GU(m1)=road_psd_rough_runway(f(m1));
% USE NEXT LINE IF SIMULTAION IS FOR SMOOTH HIGHWAY
GU(m1)=road_psd_smooth_highway(f(m1));
```

```
% USE NEXT LINE IF SIMULTAION IS FOR HIGHWAY WITH GRAVEL
%GU(m1)=road_psd_gravel_highway(f(m1));
% USE NEXT LINE IF SIMULTAION IS FOR PASTURE IN FIELD
%GU(m1)=road_psd_pasture(f(m1));
end
% Step 1: Generate N/2 random phase angles with uniform denisty
% between 0 and 2pi

TH=random('unif',0,2*pi,no2,1);

% Step 2: Generate the appropriate amplitude at each frequency using
% the random phase angles.

for m=2:no2
C=sqrt(GU(m)*N*H/2);
CTH=cos(TH(m-1))*C;
STH=sin(TH(m-1))*C;
U(m)=CTH+j*STH;
k=N+2-m;
U(k)=CTH-j*STH;
end

% Step 3: Make sure the N/2+1 value is real that the negative
frequency values
% will be the mirror image of the positive frequency values.

no2p1=no2+1;

C=sqrt(GU(no2p1)*N*H/2);

CTH=cos(TH(no2))*C;

U(no2p1)=CTH+j*0.e0;

% Make sure the zero frequency value is zero to achieve a zero mean
time series.

U(1)=0.e0+j*0.e0;
```

```
% Generate Y(t), the inverse transform of the N Fourier Transform
values Y(f).

[U]=ifft(U);

% Rescale to get the correct time series corresponding to this desired
PSD.

for m=1:N
U(m)=real(U(m)/H);
end


% Plot the PSD and time series
%PLOT OF ROAD ELEVATIONS VS TIME
t=0:H:(N-1)*H;
t=t';
U=U';
figure
plot(t,U);
xlabel('Time (sec)')
ylabel('Output


%PSD for HIGHWAY WITH GRAVEL AT VELOCITY = 60 m /sec

function[GU]=road_psd_gravel_highway(f)
N=2.1;
Csp=4.4e-6;
GU=(Csp)./(17.*(f/17).^N);
```

References

1. Chinny Yue(1986) "Control Law Designs for Active Suspensions in Automotive Vehicles", MS Thesis, Massachusetts Institute of Technology.

2. Thomas D.Gallispie, "Fundamentals of Vehicle Dynamics",*Society of Automotive Engineers.*

3. Anil,Prasad.Pravin, Kulkarni (2008)"Optimal Design of Passenger Car Suspension for Ride and Road", *Journal of the Brazilian Society of Mechanical Sciences and Engineering*.

4. Abramov, Manan, Durieux(2009) "Semi-Active Suspension System Simulation Using SIMULINK",*International Journal of Engineering Systems Modeling and Simulation*.

5. Hadi Adibi, Geoff Rideout (2010),"Bond Graph Modeling and Simulation of Full Car Model with Active Suspension" MS Thesis Memorial University, St. John's, NL, Canada.

6. Arshad Khan, Devashish Sarkar, Reshad Ahmar and Hitenkumar Patel (2011),"Random Vibration Analysis and Fatigue Life Evaluation of Auxiliary Heater Bracket", *SIMULIA India Regional User's Meeting.*

7. Carl Cheng, Jeff Crull, "Random Vibration Analysis of Dual 101 EM Assembly".

8. Secil Ariduru(2004) "Fatigue Life Calculation by RainFlow Cycle Counting Method", MS Thesis, Middle East Technical University.

9. F. Vakili-Tahami, M. Zehsaz and M.R. Alidadi(2009) ,"Fatigue Analysis of the Weldments of the Suspension-System-Support for an Off-Road Vehicle under the Dynamic Loads Due to the Road Profiles", *Asian Journal of Applied Sciences*, 2: 1-21.

10. Uzair Khan(2010), "Vehicle Suspension Control System Using Full Car Model", MS Thesis National University of Sciences and Technology.

11. German Filippini, Diego Delarmelina, Jorge Pagano, Juan Pablo Alianak, Sergio Junko and Norberto Nigro(2007), "Dynamics of Multibody Systems with Bond Graphs" *Mechanica Computacional*, Vol XXVI, pp 2943-2958, Cordoba, Argentina.

12. Kailas Vijay Inamdar(2011) "Vehicle Suspension Optimization for Stochastic Inputs" MS Thesis, University of Texas at Austin.

13. StoFlo™ Rain Flow Cycle Counting Excel Template, http://stotera.com/stoflo/.

14. Dean C.Karnopp,Donald L.Margolis, Ronald C.Rosenberg, "System Dynamics, Modeling and Simulation of Dynamic Systems", Third Edition, John Wiley and Sons,p-5.

15. Fatih Kagnici(2012), "Vibration Induced Fatigue Assessment in Vehicle Development Process", *World Academy of Sciences.*

16. ANSYS Workshop5A, "Random Vibration(Girder Assembly)".

17. Lesser, C., Thangjitham, S.and Dowling, N.E (1994), "Modeling of Random Vehicle Loading Histories for Fatigue Analysis",*Int.J.of Vehicle Design,*Vol.15.Nos.3/4/5,pp.467-483.

18. ASTM E-1049, "Standard Practices for Cycle Counting in Fatigue Analysis".

19. NWM Bishop and F.Sherratt (2000), “Finite Element Based Fatigue Calculations”, Nafems Publication.

20. Paul H.Wirsching, Thomas L.Paez, Keith Ortiz (1995), “Random Vibrations, Theory and Practice”, A Wiley-Interscience Publication, John Wiley & Sons, Inc.

21. RANDRIATEFISON Nirilalaina, “Modelling in 2D the Roughness of the Roads in the Equation of Vehicle Movement”, *5th High-Energy Physics International Conference in Madagascar* 25-31th august 2011 Antananarivo.

22. Michael R.Hatch, “Vibration Simulation Using MATLAB and ANSYS” Chapman&Hall/CRC p-123.

23. Christian Lallane(1999), “Mechanical Vibration and Shock Fatigue Damage”, Volume IV, Taylor and Francis Books, Inc.

24. Norman S.Nise(2004), “Control Systems Engineering”, Fourth Edition, John Wiley&Sons Inc p-455.